Copyright Warning & Restrictions

The copyright law of the United States (Title 17, United States Code) governs the making of photocopies or other reproductions of copyrighted material.

Under certain conditions specified in the law, libraries and archives are authorized to furnish a photocopy or other reproduction. One of these specified conditions is that the photocopy or reproduction is not to be "used for any purpose other than private study, scholarship, or research." If a, user makes a request for, or later uses, a photocopy or reproduction for purposes in excess of "fair use" that user may be liable for copyright infringement,

This institution reserves the right to refuse to accept a copying order if, in its judgment, fulfillment of the order would involve violation of copyright law.

Please Note: The author retains the copyright while the New Jersey Institute of Technology reserves the right to distribute this thesis or dissertation

Printing note: If you do not wish to print this page, then select "Pages from: first page # to: last page #" on the print dialog screen

ABSTRACT

RECOVERY OF VALUABLE METALS FROM SPENT LITHIUM-ION BATTERIES USING ORGANIC ACIDS: ASSESSMENT OF TECHNO-ECONOMIC FEASIBILITY

by
Leqi Lin

Lithium ion batteries (LIBs) are used in diverse electronic products with anticipated over 500 thousand tonnes of the waste LIBs globally in 2020. To protect the environment and also recover valuable materials such as lithium (Li) and cobalt (Co), our research employed a hydrometallurgy method and demonstrated that exposure of spent LIBs to Organic Aqua Regia (OAR) could leach Li and Co without the pre-separation of cathode from Al foil using organic solvents such as Dimethylformamide (DMF) and N-Methyl-2-pyrrolidone (NMP). The leaching efficiency of 99% and 94% for Li and Co were obtained with a leaching rate of 0.021, 0.167 $mg \cdot mg^{-1} \cdot h^{-1}$ respectively. Furthermore, our life cycle assessment (LCA) indicates that OAR could reduce 65% greenhouse gas (GHG) emission compared to extraction from natural mines or reduce 26% GHG emission compared to pyrometallurgy and hydrometallurgy processes with sulfuric acid.

RECOVERY OF VALUABLE METALS FROM SPENT LITHIUM-ION BATTERIES USING ORGANIC ACIDS: ASSESSMENT OF TECHNO-ECONOMIC FEASIBILITY

by
Leqi Lin

A Thesis
Submitted to the Faculty of
New Jersey Institute of Technology
in Partial Fulfillment of the Requirements for the Degree of
Master of Science in Civil Engineering

John A. Reif, JR. Department of Civil and Environmental Engineering

May 2020

APPROVAL PAGE

RECOVERY OF VALUABLE METALS FROM SPENT LITHIUM-ION BATTERIES USING ORGANIC ACIDS: ASSESSMENT OF TECHNO-ECONOMIC FEASIBILITY

Leqi Lin

Dr. Wen Zhang, Dissertation Advisor Associate Professor of Civil and Environmental Engineering, NJIT	Date
Dr. Lucia.Rodriguez-Freire, Dissertation Co-Advisor Assistance Professor of Civil and Environmental Engineering, NJIT	Date
Dr. Taha F Marhaba, Committee Member Professor of Civil and Environmental Engineering, NJIT	Date
Dr. Eonsoo Lee, Committee Member Associate Professor of Mechanical and Industrial Engineering, NJIT	Date

BIOGRAPHICAL SKETCH

Author: Leqi Lin

Degree: Master of Science

Date: May 2020

Undergraduate and Graduate Education:

- Master of Science in Civil Engineering,
  New Jersey Institute of Technology, Newark, NJ, 2018

- Bachelor of Science in Earth and Environmental Science,
  National Chung Cheng University, Chiayi, Taiwan, 2017

Major: Civil Engineering

Presentations and Publications:

Leqi Lin, Wen Zhang*, 2020 recovery of valuable metals from spent lithium-ion batteries using organic acids: assessment of techno-economic feasibility, resources, conservation and recycling. (preparing)

Leqi, Lin, Wen Zhang, "Leaching of valuable metals from spent-lithium-ion batteries (LIBs) using Organic Aqua Regia,"., ACS American Chemical Society 259th National Meeting, Pennsylvania Philadelphia, March 23th, 2020.

Leqi, Lin, Wen Zhang, Leaching of valuable metals from Lithium-ion batteries (LIBs) using green organic acids, Graduate Student Research Day, New Jersey Institute of Technology, NJ, 2019.

Leqi, Lin, Wen Zhang, Leaching of valuable metals from Lithium-ion batteries (LIBs) using green organic acids, EAS The Eastern Analytical Symposium and Exposition, Princeton, NJ, Oct 15th, 2019.

Leqi, Lin, Wen Zhang, Green chemical process to recovery Li and Co from spent Lithium-ion batteries, WEA NJ annual conference student poster contest, Atlantic City, May 7th, 2019.

ACKNOWLEDGEMENTS

These years as a master's student at NJIT are a splendid and fast-paced experience of my life. Deep appreciations fill in my mind. Here I would like to mention those people who offered help, support, and unforgettable experiences for me these years.

First and foremost, I would like to express my special gratitude to Dr. Wen Zhang, my research advisor and mentor for his invaluable guidance and support throughout my graduate journey. I appreciate Dr. Zhang to provide the opportunities being a research assistant, which not only financially supported my study here but also offered a great research area that I feel fortunate to learn about. He always encourages me to join different professional conferences and attend student presentation or poster competitions, apply the scholarships and mentor other students. He has been an amazing role model for me during my graduate work and constantly motivates me to pursue further achievement. His mentorship positively influences me and helps me build confidence for research and future career. Thank you for the tireless encouragement, unparalleled opportunities and for pushing me forward throughout the year which has helped me grow up as a researcher.

Special thanks to my dissertation committee members, Dr. Eonsoo Lee and Dr. Lucia Rodriguez-Freire. I appreciate for their precious time in their busy schedules to review my thesis and provide me constructive and critical comments. I would also want to thank the finical support that makes the dissertation possible. We are thankful to the EPA Pollution Prevention (P2) grant (Grant No. NP96259118), the NJIT Undergraduate Research

Innovation (URI) phase I and II grants (2018 fall), 2018 NAME Green Technology Scholarship and Suez company, which provides funding opportunities to support my research and studies.

I would further want to extend my gratitude to Dr. Li-Kun Hua, who completes major parts of the grant proposal to EPA. Without his indispensable contributions and advice, I would likely spend more time to complete my thesis. I also want to thank Dr. Yu-Jen Shih, spent his precious time to provide me many practical and useful information on my experiment. His promptly replies to my queries always made me feel warm and optimistic during the hard time. Mrs. Ying Yao, the chief chemist of Meadowlands Environmental Research Institute (MERI) at Rutgers University taught me the principles of ICP-MS and basic experimental skills. Besides, Mrs. Yao is also tender and kind-hearted, and gave me a ride home every time after I finished the analysis at MERI. Thank you for the precious time again. Suez company, Dr. Cheng-yue Shen, taught me the design ability and viewpoint for the project through the cooperation.

In addition, I received a lot of help from the professors and students in NJIT and Rutgers. I want to thank Professor Eon-Soo Lee, my teacher of course of introduction to fuel cells and batteries. The course inspired me with abundant knowledge related to the concept of my thesis such as electrochemistry, and the structure of batteries. Dr. Hsin-Neng Hsieh and Dr. Fadi A. Karaa, my academic advisors, advised me on the course selection since I came to NJIT. For my current group members, the Ph.D. candidate Xiaonan Shi,

also game immense support (e.g., offered to help when I needed to join the conference 2-3 hours far away from where I lived), and also advised me a lot on the projects; Dr. Likun Hua, as I mentioned above, aided in the EPA proposal that becomes my thesis topic now. The Ph.D candidate, Qingquan Ma, always helps me prepare the dangerous chemicals and a good listener when I have doubts toward the future and experiment. The Ph.D candidate Chunzhao Chen and Dr. Wanyi, Fu, are all exemplary persosn for me to learn from.

Moreover, my friends, Jiaheng Zhang, Zhonghao Li, Shuyue Yang, Peiran Jia, Qi Meng and Zixia Meng encourages and accompanies me when I feel stressful. They took care of me when I was sick, cooking delicious cuisine and cakes on the festival. They are my family in the United Stated, and also the friends forever even we may separate in different places someday.

Last, but not the least, I want to thank my mother for her unconditional wait and support. Without her understanding and encouragement, I would not have this chance to experience this 2-year wonderful journal. Every time I miss her and the cuisine in my hometown, she sent me a box of cookies, Chinese traditional cakes and instant noodles at once. When she traveled abroad, she sent me a lot of souvenir every time. Appreciation for my uncle, thank you for taking good care of my mother and my cats for these years. Dr. Hsuehyu Lu, my academic and research advisor when I was an undergraduate student, he played a role of my father to receive my pessimistic.

TABLE OF CONTENTS

Chapter **Page**

LIST OF TABLES

LIST OF FIGURES

CHAPTER 1

INTRODUCTION

1.1 Background of Lithium Ion Battery

In 1800, Alessandro Volta invented the first battery was invented by stacked copper (Cu) and zinc (Zn) as anode and cathode. In 1836, the first rechargeable based on lead acid was invented by the French physician. For the pursuit of instability and maximum stored energy needed for the electronics markets (mobile phone and laptop computer), nickel-cadmium battery (NiCd) and nickel-metal hydride batteries which had longer life than NiCd were then invented successively around the early 20^{th}. New battery technologies usually require higher energy capacity, higher power/energy density, longer storage life, low self-discharge rate and thermostable rechargeable batteries based on new advanced materials. The traditional rechargeable batteries (lead acid, NiCd and nickel-metal hydride) face limitations in their energy densities (80-300$Wh \cdot L^{-1}$).[1] To increase the energy densities, the $LiCoO_2$ (LCO) type of cathode materials was developed by Goodenough et al. in 1979[2], followed by lithium-ion batteries (LIBs) that were commercialized by SONY in 1991.[3] Basically, LIBs are based on different redox-oxygen reactions between anode and cathode, which generate cell voltages typically in the 1.0 to 4.2 V range. Lithium (Li) is the most electropositive element allowing Li based batteries to have the higher energy density storage (250-693 $Wh \cdot L^{-1}$) with a transition metal, such as cobalt (Co), nickel (Ni),

manganese (Mn) and iron (Fe) to compensate for the charge when the Li-ion arrives or departs.

LIBs owing to the unmatchable high energy and power density have been widely used in portable electronic products, such as mobile phones, laptops, automobiles, and cameras.[4] The use of LIBs is expected to expand to meet the rising demand especially for energy storage devices such as solar and wind and for electric vehicles. However, there are limited countries that possess exploitable deposits of cobalt (65% in Congo, Canada, China and Russia),[5] and the price of cobalt is about 4.7 times more expensive than nickel, 6.6 times more expensive than titanium and 7 times more expensive than lithium.[6] The global LIBs market size was valued at $37.4 billion in 2018, advancing at a 16.2% CAGR to at $ 92.2 billion by 2024.[7, 8]In Middle East and Africa, the market of LIBs in 2016 was valued over $1 billion,[9] where the China market will have a dramatic gain of over 13% by 2025 with its strong economic growth along with ongoing expansion and development of automobile manufacturing. According to the GSMA real time intelligence data, there are 5.17 billion people that have a mobile phone device, and is predicted to increase to 7.33 billion by 2023.[10] Furthermore, over 20% of vehicles in the United Stated will be replaced by electrical vehicles by 2030 that may use LIBs as fuel sources. As a result of the intensive use of LIBs, there is a predicted shortage of lithium and other transitional metals in LIBs due to the lack of effective recovery or recycling processes of LIBs.[1112] The recovery of

spent-LIBs is thus beneficial to the environmental protection and also conservation of strategically important materials.[13, 14]

Approximately 500 thousand tons of spent-LIBs will be produced globally in 2020 from 25 billion units of spent-LIBs.[15] The typical life span of LCO-type LIBs is around 1-2 years (500-1000 cycles) depending on the usage condition and the quality of the battery. Among these spent LIBs, most of them are LCO type LIBs, and around 100,000 tonnes are available for recycling and recovery. The residues of spent-LIBs contain high metals concentration levels, which could result in environmental pollution if not properly managed.[16] . Since 2016, the Department of Defense (DoD) released a climate change on military installations located around the world. The DoD released a $5.5 million funding opportunity announcement (FOA) to develop new technologies to profitably capture 90% of LIBs in the United States. Li as the medium-term critical materials due to the rapid increases in market penetration projected for electric vehicles using LIBs, which increases the importance of Li as clean energy. The United States needs to construct the dependence on the critical materials which mostly from foreign countries, thus the goal of FOA is to develop new innovative solutions to collecting, storing, and transporting spent-LIBs.

Conventional recovery of cathode materials involves time-consuming, complicated pretreatment and high temperature calcination. Moreover, the use of inorganic acids such as sulfuric acid (H_2SO_4) [17, 18],hydrochloride acid (HCl) [19, 20] and nitric acid (HNO_3) [21, 22] may cause negative effects on the environment and human health due to the penetration of

leaching residue into the eco-system and toxic emissions such as Cl_2, SO_3 and NO_x.[17, 23] Recently, many studies propose the use of green chemicals or regents, such as citric acid[24, 25], succinic acid[26] and malic acid,[27, 28] for the leaching process to dissolve cathode elements to be recovered. Nearly 99% Li and over 90% Co can be achieved using citric acid and DL-malic acid.[25, 29] Golmohammadzadeh et al.[16] reported the leaching efficiency between citric acid, DL-malic acid and acetic acid with ultrasonic agitation, an optimizing effect of 99.80% of Li and 96.46% for Co can be recovered by citric acid at 5 hrs. M. Roshanfar et al.[30] proposed 100% of Li and 97.36% of Co recovery efficiency under optimized leaching condition (Temperature of 79°C, 16.3 $g \cdot L^{-1}$ pulp density, 165 mM H_2O_2 with 1.52M lactic acid for 2 hrs.) The limitation of hydrometallurgy method with organic acids originates from weak acid which referring to the lower ability to release hydrogen ion into solution when reacting. This causes a relatively lower pulp density which means a great amount of leaching solution input, and further increases the input of H_2O_2 and temperature than inorganic acid. Furthermore, conventional hydrometallurgy method is hindered by the complicated pretreatment processes.

1.2 Components and Industrial Application for Lithium-Ion Batteries

1.2.1 Principles and Classification of Lithium-Ion Batteries

Figure 1.1 shows the major principle of charging and discharging processes of LIBs. During the discharging or electricity generation process, the lithiated graphite (Li_xC_6)

anode undergo an electrochemical reaction to release Li^+ ions that migrate through the electrolyte to the delithiated cathode.[31] During the charging process, the reverse process occurs by applying external power sources (e.g., a DC power) that electrons flow to anode to attract Li^+ ions released from cathode and cause the formation of lithiatiation on anode material.

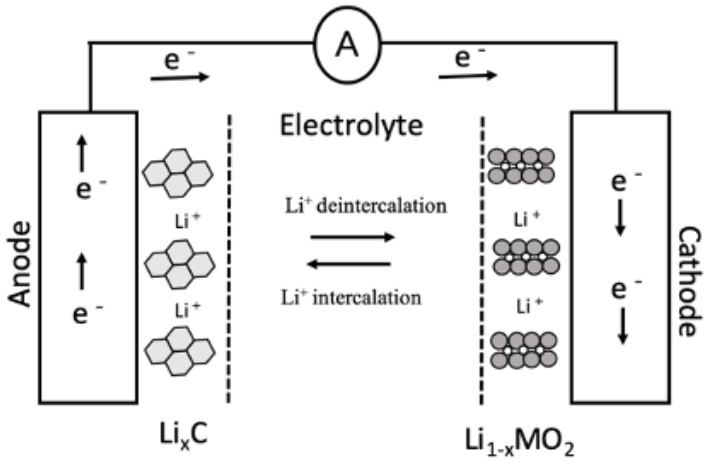

Figure 1.1 The schematic of lithiation and delithiation inside the charged Lithium-ion batteries when discharging.

LIBs can be first classified into different shapes as coin, cylindrical and prismatic according to the current manufacturing practices. The prismatic shape can be further divided into hard-case and pouch based on the housing stability.[32] The cylindrical shape batteries are typically assigned five-digit numbers, where the first two digits are the approximate diameter in millimeters, followed by the last three digits indicating the approximate height in tenths of millimeters.[33] For example, 18650 cylindrical shape batteries have typical capacity range from 1500-3600 mAh with a diameter in 18 mm and a length in 65 mm.

1.2.2 Components for Lithium-Ion Batteries

LIBs consist of electrolyte for ion transfer, anode, cathode, and separators that prevent short circuiting as shown in **Figure 1.2**.[34] **Table 1.1** shows the average mass distribution of these components for LCO type LIBs with the total weight of 18.74 g for a single unit.[4]

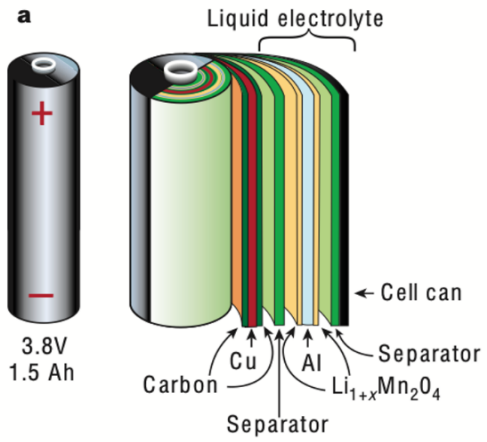

Figure 1.2 Typical structure of an 18650 LIB.

Source:[35]

Table 1.1 Average Material Content of Portable LCO Type LIBs

Battery component	Product data sheet in mass-%
Casing	20-25
Cathode material ($LiCoO_2$)	25-30
Anode	14-19
Electrolyte	10-15
Copper foil	5-9
Aluminum	5-7
Separator	-

Source:[36]

1.2.2.1 Anode Materials

Currently, the two most common used anode materials are carbon (graphite) and lithium alloyed metals.[37] Graphite consist of sheets packed in hexagonal (AB) or rhombohedral

(ABC) arrangements as shown in **Figure 1.3** Due to the low cost of graphite manufacturing and favorable electrochemical characteristics, the carbon-based anodes are the key anode material in the development of LIBs. The use of a layered carbon-graphite anode can store Li ions between the carbon atoms (in a process called intercalation) during charging and release them during discharging, however the formation of dendrites causing the short-cut and instability for LIBs. The anode of all 18650 LIBs are basically the same in composition, containing carbon-silicon and graphite as the active material, PVDF binder, additives and conductor coating on copper foil.[37]

Besides graphite, lithium alloy anodes such as lithium aluminum (Li-Al) and $LiTiO_2$ are also important anode materials for LIBs.[37] Li-Al is the first to be developed as anode for LIBs with a theoretical capacity of 2235 $mAh \cdot g^{-1}$, which is much larger than that of graphite (372 $mAh \cdot g^{-1}$).[38] $LiTiO_2$ is another anode material with excellent electrochemical cycling since it does not show any volumetric changes during lithiation and dilithiation processes.[39, 40] The metals found in the graphite intercalation alloy protects the inserted Li, making it less reactive towards electrolytes. Moreover, great advantage for lithium titanium is its ability for the fast-charging application.[41]

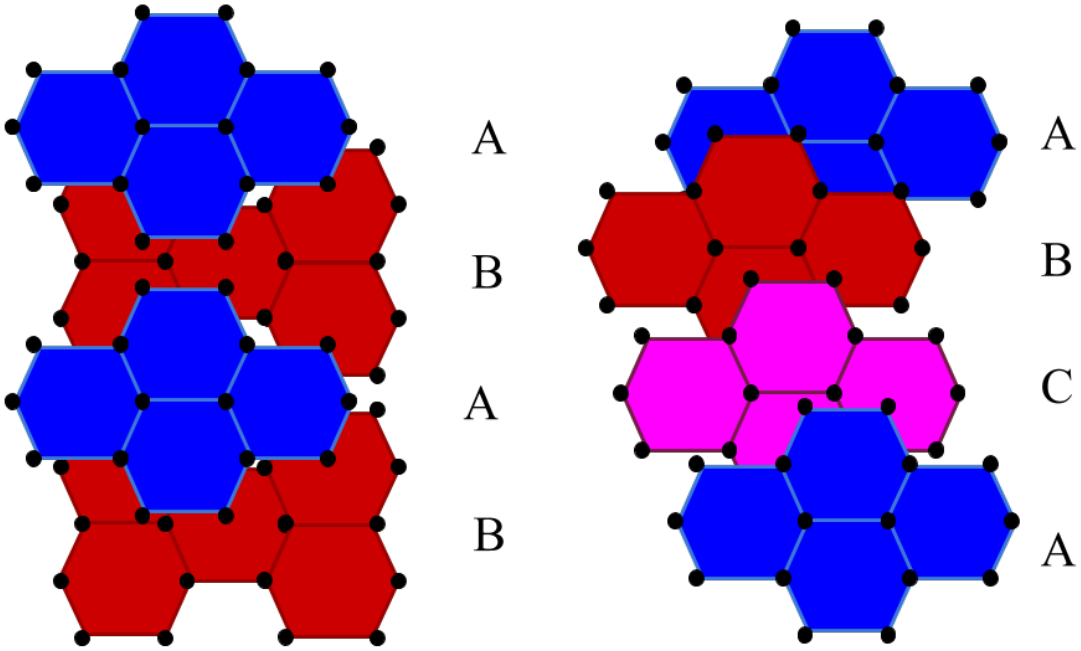

Figure 1.3 Crystal structures of two modifications of (a) Hexagonal; (b) Rhombohedral graphite.

1.2.2.2 Cathode Materials

Table 1.2 shows the typical element compositions for cathode of LIBs. The cathode is usually composed of the active materials such as Lithium Cobalt Oxide ($LiCoO_2$, LCO), Lithium Nickel Manganese Cobalt Oxide ($LiNiMnCoO_2$, NMC), Lithium Manganese Oxide ($LiMn_2O_4$, LMO), Lithium Iron Phosphate ($LiFePO_4$, LFP) and Lithium Nickel Cobalt Aluminum Oxide ($LiNiCoAlO_2$, NCA).[4] Depending on the atomic arrangement or crystal structures , these five cathode materials can be categorized into layer LCO, LMO, NCA, spinel LMO and olivine LFP as shown in **Figure 1.4. Table 1.3** compares the fundamental properties and applications between different cathode materials.

Table 1.2 Composition of LCO Type Active Cathode Material

Cathode material	Mass percentage-%
Co	45.1
Li	6.3
Al	0.67
Mn	11.8
Ni	0.3

Source: [42]

Table 1.3 Cathode Component of Lithium Ion Batteries and Each Application

Type	LCO	NMC	LMO	LFP	NCA
Voltages (V)	3.0-4.2	3.0-4.2	3.0-4.2	2.5-3.65	3.0-4.2
Energy density ($Wh \cdot Kg^{-1}$)	150-200	150-220	100-150	90-120	200-260
Thermal Runaway (^oC)	150	210	250	270	150
Cycle life	500-1000	1000-2000	300-700	1000-2000	500
Application	Portable electronics	E-bikes, electrical vehicles	Power tools, electrical powertrains	high load currents and endurance	Industrial electric powertrain

(a) Lithium Cobalt Oxide (LCO)

LCO, as the first and the most common used cathode material in LIBs, has a layer structure with oxygen in a cubic close-packed arrangement. Due to its high energy density, LCO has been used for portable electronic equipment (mobile phone, laptops and digital cameras). After removal of Li ions, the oxygen layers rearrange themselves to give hexagonal close packing of oxygen in CoO_2. The drawback of LCO is the short-life span, low thermal stability and power density which cannot output large amounts of energy immediately.

(b) Lithium Iron Phosphate (LFP)

LFP has good electrochemical performances with low resistance and more tolerance against cell damage when charged fully if kept at high voltage for a specific time. As a trade-off, LFP has a lower nominal voltage of 3.2 V (normally 3.6V) compared with other cobalt-based LIBs. Normally, LFP is used to replace the lead acid battery in vehicles by using several cells in series to reach the similar voltage.

(c) Lithium Manganese Oxide (LMO)

LMO is one of the oldest cathode materials due to its accessibility, low cost, and high electrochemical properties. LMO has a three-dimensional spinel structure, which improves the ion conductivity and decreases the internal cell resistance and ohmic loss. Moreover, LMO spinel has high thermal stability, high rate capability (a measure of power generation), and low health and environmental impacts.[37]

(d) Lithium Manganese Nickel (NMC)

NMC is one of the most successful cathode materials that is produced by blending LMO batteries with $LiNiCoO_2$. Nickel-based systems have higher energy density, lower cost and longer cycle life relative to cobalt-based cells. NMC is also chosen to be the best batteries for electric vehicles and expected to replace other kinds of cathode materials in the years to come.

(e) Lithium Nickel Cobalt Aluminium Oxide (NCA)

NCA shares similarities with NMC with respect to high energy density, power density and long-life span. However, higher cost and safety problems (e.g., short circuit and capacity

fading) limit the market potential of NCA LIBs.[43] Usually, NCA is used for special applications such as electric powertrain by Tesla[44, 45], where aluminum empowers the battery system greater thermal stability.[46]

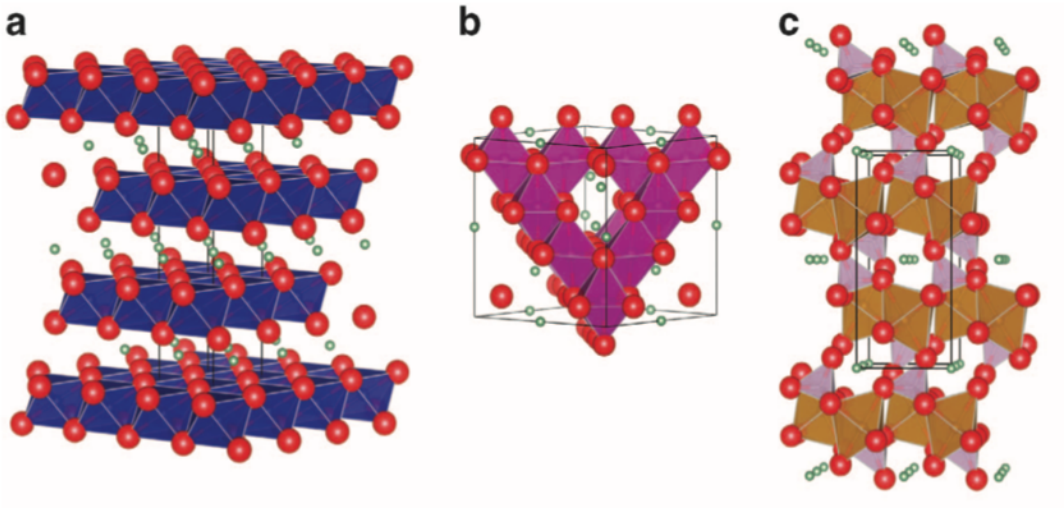

Figure 1.4 Crystal structures of (a) layered LCO, NMC, and NCA , (b) spinel LMO and (c) olivine LFP.

Source: [47]

1.2.2.3 Electrolyte

Electrolytes that have high dielectric constants are needed for ionic transportation and movement between electrodes. The electrolyte is an aqueous solvent made of organic solvent with dissolved salts, acids or alkalis. Normally, the dissolved salt solution of lithium hexafluorophosphate ($LiPF_6$) with propylene carbonate (PC) and dimethoxyethane (DME) is the common used electrolyte.[48] Besides $LiPF_6$, other salts such as $LiBF_4$, $LiCF_3SO_3$ and $LiN(SO_2CF_3)_2$ are sometimes used depending on the specific considerations

such as high ion conductivity and pave the way for future publications on polymer gel electrolytes.[49-51]

1.2.2.4 Separators

The separators are used to physically separate the anodes and cathodes and prevent the battery from explosion due to the direct contact of the two electrodes without hampering the transportation of Li ions between the pair of electrodes.[52] Typically, the separators account for 15-20% in cell component costs, whereas 20-25% accounts for cathodes and 10-15% for anodes.[53-55] Normally, the separators are made of porous polyolefin membranes such as polyethylene (PE), polypropylene (PP) or combination of PE and PP for liquid electrolyte batteries,[56] as list in **Table 1.4.**

Table 1.4 Major Separator Manufacturers

Manufacturers	Materials	Separator Design
Asahi Kasei Chemicals	Polyolefin and ceramic-filled polyolefin	Biaxially orientated
Celgard LLC	PE, PP, and PP/PE/PP	Uniaxially orientated
Entek membranes	Ceramic-filled UHMWPE	Biaxially orientated
ExxonMobil/Tonen	PE and PE/PP mixtures	Biaxially orientated
SK energy	PE	Biaxially orientated
Ube industries	PP/PE/PP	Uniaxially orientated

Source: [56]

1.3 Importance and Challenge of Resource Recovery from Spent-LIBs

1.3.1 Market Growth for LIBs

The global LIBs market size was valued at USD 37.4 billion in 2018, advancing at a 16.2% CAGR to at USD 92.2 billion by 2024.[7] In Middle East and Africa, the market of LIBs in

2016 was valued over USD 1 billion,[9] where the China market will have a dramatic gain of over 13% by 2025 with its strong economic growth along with ongoing expansion and development of automobile manufacturing. According to consultancy Cairn Energy Research Advisors, the annual global production of LIBs grew from 100 gigawatt hours (GWh) in 2017 to almost 800 GWhs in 2027.[57] The United States LIB market was also valued at over $ 6 billion in 2017 and is forecast to grow at a CAGR of more than 13% to surpass billion by 2023.[58] The major companies operating in the global LIBs market are BYD Company (China), KAS Group (China), CALB (China), LG Chem (South Korea), Panasonic (Japan) , Samsung SDI(South Korea), GS Yuasa (Japan), Hitachi (Japan), VARTA Storage (Germany) and Farasis Energy (U.S.).

1.3.2 Recovery Market Analysis

In the years to come, over than 200,000 tonnes of LIBs have reached end-of-life from applications in electronics such as mobile phones, tablets, laptops, cameras, and other portable commercial technologies.[59] As shown in **Figure 1.5a,** in 2018, 70% of spent LIBs of about 97,000 tones were processed in China for recovery or recycling and 19% of spent LIBs (about 23000 tonnes) was processed in South Korea. In Australia, only 2 percent of the country's 3300 tonnes of lithium-ion waste was recycled. Most of spent LIBs ended up in landfill without proper disposal, which creating important market for material companies recycle and recover the LIBs[59]. Among these spent LIBs, most of them are LCO type LIBs,

and around 100,000 tonnes are available for recycling and recovery, as shown in **Figure 1.5b** and **Figure 1.5c.** As demonstrated by its cycle life, LCO batteries are greatly limited with its low life span (around 1-2 years), which is not as long as batteries current used in vehicles or other industrial applications. Accordingly, the quantity and weight of discarded LIBs in 2020 can surpass 25 billion units with 500 thousand tonnes[60], potentially causing environmental problems if not properly managed. Moreover, for countries that lack the key raw materials such cobalt in the Democratic Republic of the Congo[5], recovery from spent LIBs is also an opportunity to reduce the import and dependence of raw materials from other countries. Since 2016, the Department of Defense (DoD) released a climate change on military installations located around the world. The DoD released a $5.5 million funding opportunity announcement (FOA) to develop new technologies to profitably capture 90% of LIBs in the United States. The United States needs to construct the dependence on the critical materials which mostly from foreign countries, thus the goal of FOA is to develop new innovative solutions to collecting, storing, and transporting spent-LIBs. In U.S., the company of American Manganese holds two patents with the ability to recover over 99% of valuable metals from NMC, LCO and NCA types of cathode materials. In Europe, Umicore claimed that their pyro-metallurgical combined with hydro-metallurgical process can use to recover mix-types of cathode materials with 80-100% recovery rate.[61] There are recycling programs for LIBs in several countries, such as the U.S., Canada, South Korea, Japan and China, most of which exploit pyrometallurgical processes in metals recovery.

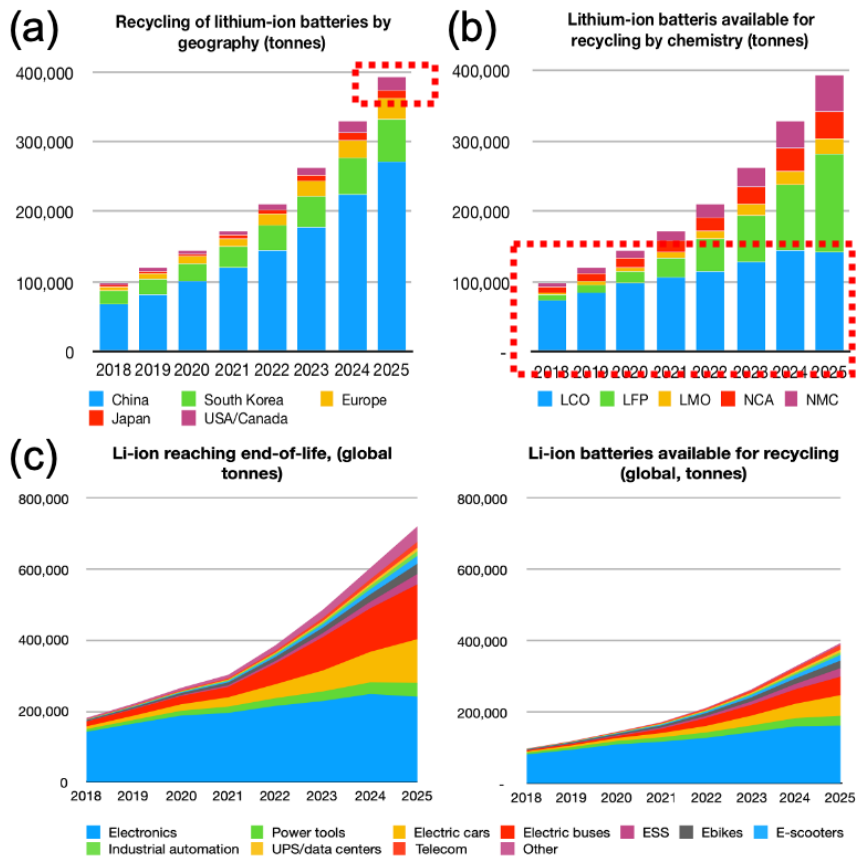

Figure 1.5 The recycling of LIBs from (a) countries, (b) available market share of ongoing different cathode materials and (c) varied applications when reaching end-of-life.

Source:[[59]]

1.3.3 Safety Consideration and Environmental Impact

According to life cycle analysis (LCA)[62] and material flow analysis (MFA),[63] the life circulation for LIBs contains product life cycle (selling, storage, use, reuse, giving and export) and product end-of-life (recycling, landfilling and incineration).[64] Though the 2010 US Geological Survey report indicates that Li is not likely to cause serious environmental concerns Li is part of aquatic and terrestrial environments in low concentrations (100-200 ppb),[65] excessive Li pollution into waterbody and soil may cause damage to animals and

plants with over intake. Besides Li, Co in LIBs is beneficial for humans in lower concentrations because it stimulates the production of red blood cells. High concentrations of Co may compromise human health including vomiting and nausea, and vision and heart problems. The International Agency for Research on Cancer reported that cobalt is carcinogenic in high concentrations exposure (e.g., 0.3-3 $mg \cdot m^{-3}$).[66]

The cost of metal recovery from spent LIBs could be compensated by the reduced health and environmental risks. For instance, to reclaim one ton of lithium, 28 tons of batteries to be recycled, much lower than the use of 1250 tons of earth that are needed.[5] Additionally, the mining process usually releases contaminants into soil, rivers and air contamination. For example, South American depletes 500,000 gallons of fresh water, 65% percent of the region's water, to extract one ton of Li during the evaporation of the mineral-rich brine every 12-18months.[67] This intensive water consumption endangers the local farming activities, communities and sustainable development of economy. In China, Australia and North America, the traditional mining methods and chemical extraction are still used, which causing hundreds of died fish, animal and human health in the downstream from a Li processing operation. Thus, it is imperative to develop new policy and incentives mechanisms to foster the growth of technologies and economies of metal recovery from spent LIBs and recycling programs.

1.3.4 The Need for Green Chemistry

Inorganic acids such as H_2SO_4[17, 68, 69] and HNO3[21, 22] are widely used in metal leaching of solid wastes including spent-LIBs due to the high leaching efficiency and low cost. However, inorganic acids are clearly corrosive and hazardous during handling and disposal. For instance, these strong acid leachant release toxic and corrosive gases during the leaching process. Considering the importance of source pollution reduction and pollution prevention, it is necessary to develop green chemical processes to recover metals present in the cathodes of spent-LIBs. In recent years, natural organic acids are increasingly used as leachant to avoid adverse environmental impacts. For instance, citric acid ($C_6H_8O_7$) is the cheap and environmentally benign acid with excellent leaching ability.[70-72] Succinic ($C_6H_6O_4$) is also demonstrated as a leachant suitable for the sustainable recovery of Mn, Li, Co and Ni from spent-LIBs.[26] Similary, malic ($C_4H_6O_5$), aspartic ($C_4H_7NO_4$), and ascorbic ($C_6H_8O_6$) acids were also explored for metal recovery from spent-LIBs[28, 70, 73] as summarized in **Table 1.5**. Most of the studies focused on the recovery of Co and Li from cathode. Compared with the inorganic acids, these organic acids could be recovered and reused with low secondary pollution. In addition, there are fewer toxic gases release and less waste acid (through reuse) with similar or higher leaching efficiencies of Li or Co. The development of cost-effective metal recovery methods is limited by many factors such as the compositions of cathodes in LIBs (often proprietary to the public). The variations on

the physiochemical properties of different acidic leaching solutions also affect the metal recovery efficiencies.[74]

Table 1.5. Summary of the Reaction Conditions and Efficiency for Leaching Valuable Metals from Spent-LIBs

Ref.	Type of LIBs	Acid	Temp (°C)	Pulp density ($g \cdot L^{-1}$)	Time (hr)	Efficiency (%)
[19]	LCO	4M HCl	80	-	2	Li: 97, Co:99
[20]	NCA	4M HCl	90	50	18	Li, Ni, Co, Al: 100
[21]	LCO	1M HNO_3	80	20	1	Li, Co: ~100
[22]	LCO	1M HNO_3	75	20	1	Li, Co: 95
[18]	LCO	2M H_2SO_4	75	100	1	Li: 99, Co:70
[75]	Mixed	1M H_2SO_4	95	50	4	Li: 93, Co: 66
[68]	Mixed	2M H_2SO_4	95	20	4	Li: 97, Co: 92
[69]	LFP	2.5M H_2SO_4	60	100	4	Li: 97, Fe:98
[24]	LCO	1.5M Citric acid	90	30	2	Li:98, Co:96
[29]	LCO	1.5M DL-malic acid	90	20	0.67	Li:~100, Co:>90
[26]	LCO	1.5M Succinic acid	70	15	0.67	Li: >96, Co:~100
[76]	LCO	1.5M Oxalic acid	80	50	2	Li, Co: >98
[77]	LCO	1.25M Ascorbic acid	70	25	0.5	Li: >98, Co: >95
[13]	LCO	1.5M Aspartic acid	90	10	2	Li, Co: >60
[77]	NMC	1.5M TCA	60	50	0.5	Li: 99, Co: 92

1.4 Pretreatment Process for the Cathode Materials

To effectively leach metals from cathode materials, certain pretreatment must be performed on spent LIBs to expose cathode to leachant. The pretreatment generally include solvent dissolution[24, 78-81], sodium hydroxide dissolution, thermal treatment, mechanical separation and ultrasonication separation which incorporates chemical, physical, thermal and mechanization agitation to break down the organic binder structure of LIBs that attach cathode to the aluminum (Al) foil.

1.4.1 Solvent Dissolution Method

Solvent dissolution uses organic solvents to break the adhesion of the binder of cathode scraps to detach the cathode materials from the Al foil as shown in **Figure 1.6.**[78-81] In general, N-methyl pyrrolidone (NMP) is usually chosen to dissolve the polyvinylidene fluoride (PVDF) binder. After discharge and dismantle of LIBs, the cathode scraps are submerged into the NMP solution at the temperature below 100 ^{o}C (The vapor point of NMP is 202 to 204 ^{o}C) for 1 hour.[24] This process will separate cathode materials and graphite from the Al foil without changing the Al state. Zhou et al. chose dimethylformamide (DMF) to dissolve the PVDF binder using the ratio of cathode scrap and DMF of 1:1.5 ($g \cdot mL^{-1}$) in a water bath of 70 ^{o}C for stirring 2h with low cost, high solubility and reusability.[82] DMF and NMP are sometimes less effective on other chemically resistant binders such as Polytetrafluoroethylene (PTFE). Zhang et al. successfully employed trifluoroacetate (TFA) to dissolve PTFE binders and separate the cathode materials from the Al foil under mild temperature conditions.[83] The use of these organic solvents in pretreatment of spent LIBs not only increases the recovery cost but also cause other environmental concerns as these solvents or leachants may contain toxic and flammable substances requiring special disposal according to NJDEP regulation.

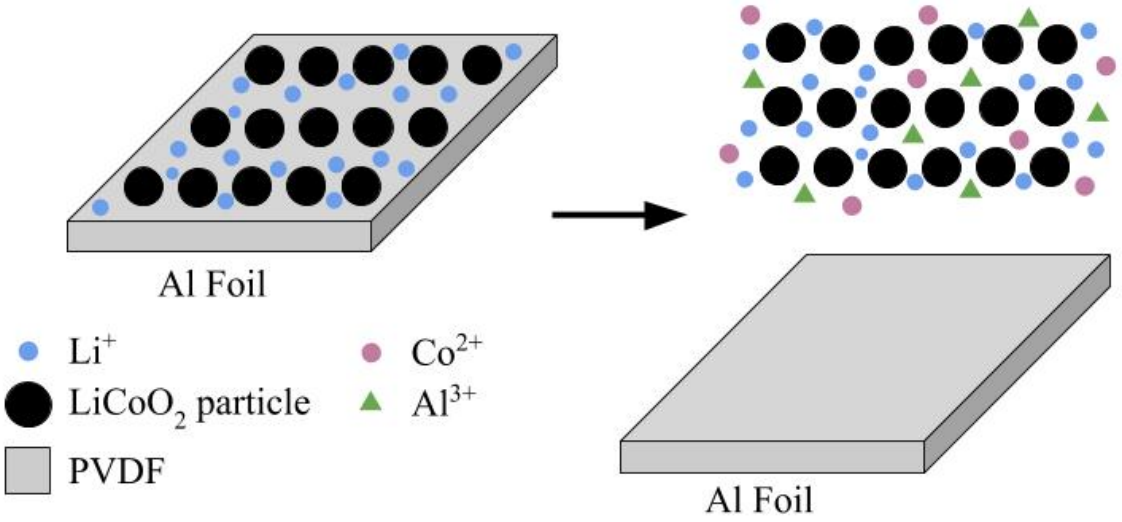

Figure 1.6. Illustration on the separation process of the cathode material and Al foil in the cathode scraps.

1.4.2 Sodium Hydroxide Dissolution Method

As shown in **Figure 1.7,** sodium hydroxide (NaOH) can also be used to separate the cathode materials from the aluminum foil.[84-88] Nan et al. separates the $LiCoO_2$ cathode materials from Al foil by adding 10 wt. % concentration of NaOH at the solid-liquid ratio of 100 g · L^{-1}.[88] After 5 hours of incubation under room temperature, the cathode materials were separated by filtering the NaOH solution with over 98% of the Al foil dissolved in the NaOH solution following the reactions in **Eq. (1.1)** and **(1.2).**[86] The residues collected on filters are heated in a furnace with a heating temperature around 150 ºC to evaporate the water to get the LCO powder. D.A. Ferreira et al. found that NaOH can selectively dissolve Al without changing the integrity of LCO cathode or significantly inducing the dissolution of Li or Co.[86] The temperature of the leaching solution does not show a significant effect

on the dissolution of Al with variations from 40%-60% as the temperature changes from 30 to 70°C.[84]

$$Al_2O_3 + 2NaOH + 3H_2O \rightarrow 2Na[Al(OH)_4] \quad (1.1)$$

$$2Al + 2NaOH + 6H_2O \rightarrow 2Na[Al(OH)_4] + 3H_2 \quad (1.2)$$

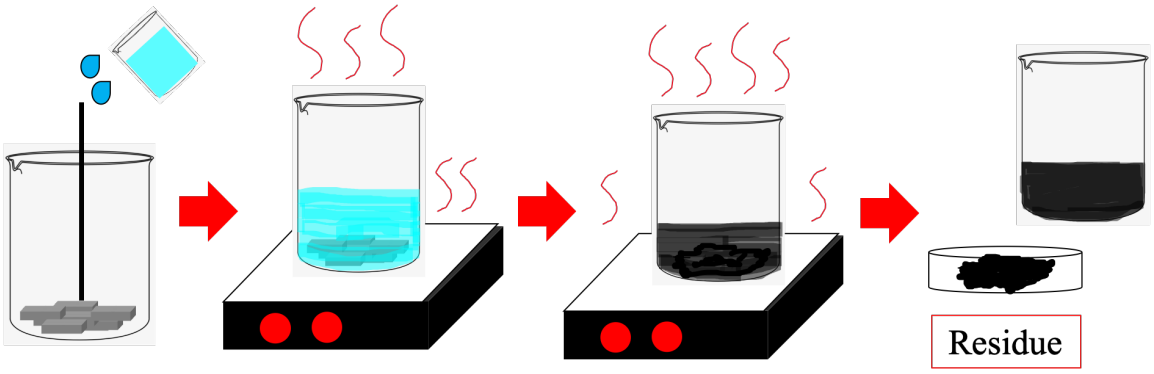

Figure 1.7 Illustration of a dissolution process using NaOH**.**

1.4.3 Ultrasonication Separation Method

Ultrasonication separates cathode materials from aluminum foil via a cavitation effect of the ultrasonic wave, which can generate localized pressures or heating to destroy insoluble substances as shown in **Figure 1.8**. Li et al. separated cathode materials (LCO) from the Al foil in a liquid container under ultrasonication of 40 Hz and 100 W, respectively.[89] Li *et al*. investigated the Sonication-assisting solvent dissolution and established a positive relation of the peel-off efficiency at 60°C temperature.[90] After filtration and drying with 120°C for 24h, a heat treatment of the collected cathode under 500-700 °C is also needed to eliminate remaining carbon (i.e., graphene) and PVDF binder.

Moreover, ultrasonication has been investigated to enhance the leaching efficiency of valuable metals from spent-LIBs.[4, 89, 90] Ultrasonication causes cavitation in a liquid, where microbubbles are generated.[91, 92] Li et al. separated the cathode materials from the Al foil in an ultrasonic washing container with agitation, with an ultrasonic frequency and electric power of 40 Hz and 100 W, respectively.[89]

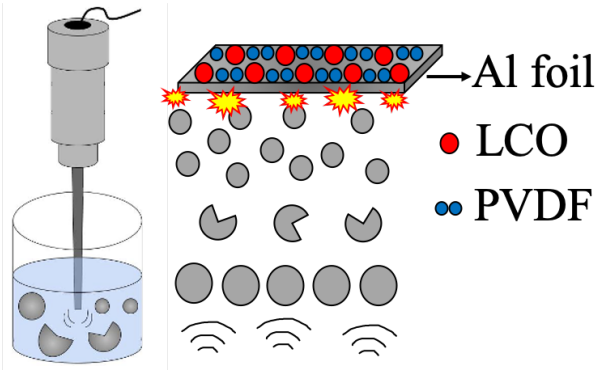

Figure 1.8. The schematic of ultrasonication in the separation of cathode materials from Al foil.

1.4.4 Thermal Treatment Method

Thermal treatment reduces the cohesion of the coated carbon black and the adhesion between cathode materials and the foil.[93] As shown in **Figure 1.9**, cathode materials are heated 350-800 ℃ in furnace to decompose most organic binders. Toxic gases such as hydrofluoric acid (HF) are released and collected by air scrubber. A vacuum pyrolysis operating below 1kPa at a temperature around 600℃, depending on the type of binder, is also used to facilitate the evaporation of the organic binder.[76, 93] Yang et al. adopted the furnace heating under high purity nitrogen gas (>99.999%) purging to completely remove

air, which also facilitated the removal of organic binders (e.g., PVDF and PTFE) compared to the vacuum pyrolysis.[94]

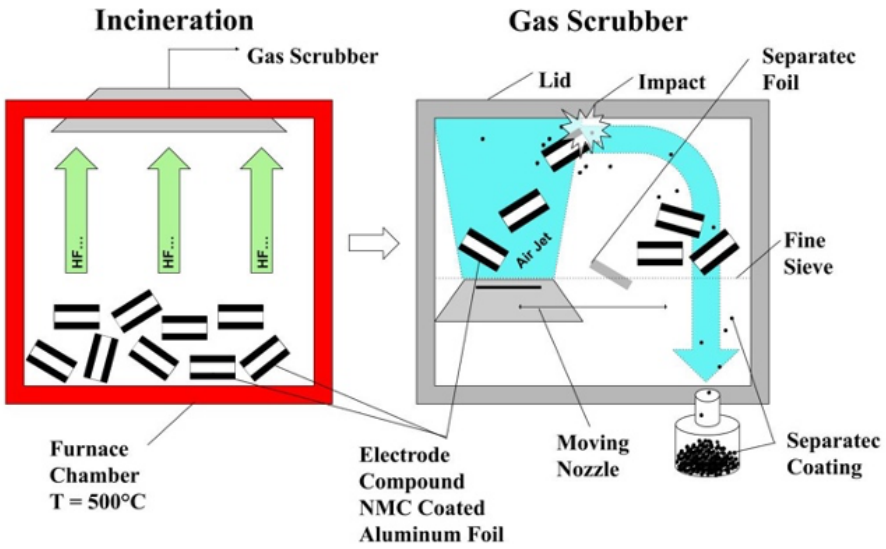

Figure 1.9 The schematic of thermal treatment (reproduced from Ref. [85] with copyright permission).

Source: [85]

1.4.5 Mechanical Separation Method

Mechanical separation replies on physical properties of materials (e.g., size, specific gravity, magnetism and electrostatic conduction) to accomplish the desired separation of components.[95] **Figure 1.10** shows the typical mechanical separation processes of crushing, removing, housing, skinning, shredding, shearing and sieving. Zhang et al. divided the crushed cathode materials into Aluminum-enriched fraction, Cobalt and Aluminum-enriched fraction and Cobalt and Graphite-enriched fraction.[96] Shin et al. demonstrated the commercial mechanical separation of crushing, sieving and magnetic separation in an

automated machine process to separate LIBs.[97] Besides mechanical methods, forth flotation which can separate the materials based on the differences between particle hydrophobicity (e.g., hydrophobic graphite and hydrophilic cathode materials) as shown in Fig.1.11.[9899] Zhan et al. also proposed the traditional froth flotation with the feed of mixing materials in response to the various types of cathode materials for the separation of graphite and cathode materials.[100] Though mechanical separation is simple to operate, the decomposition of $LiPF_6$ generates HF and POF_3 during the separation, which raises environmental concerns.

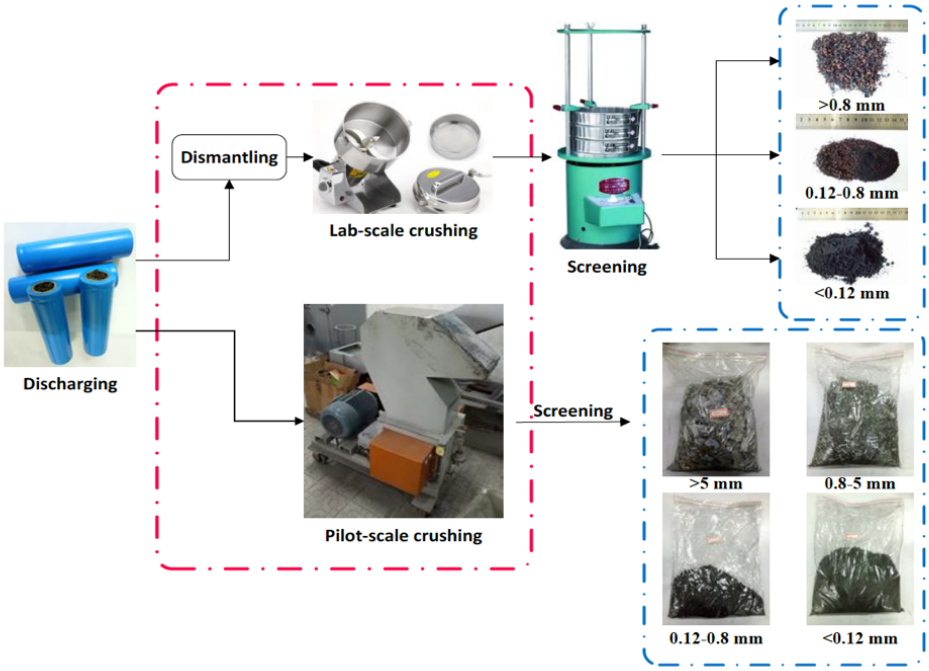

Figure 1.10 Flowsheet for mechanical separation of recycling spent-LIBs.

Source:[101]

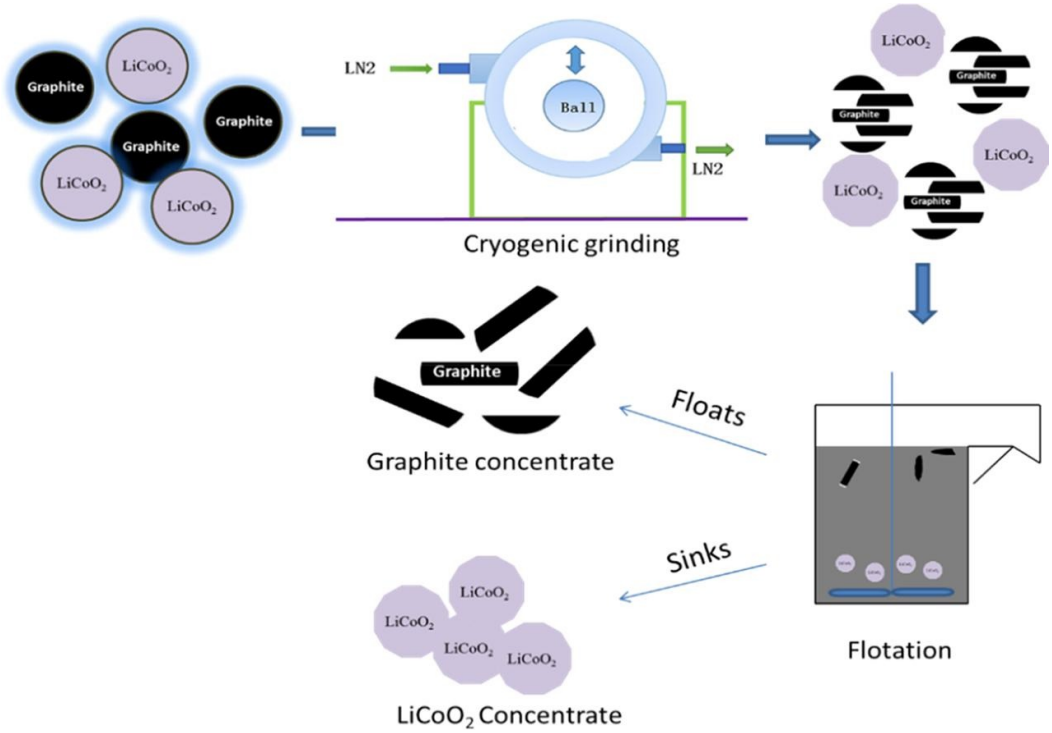

Figure 1.11 Illustration of froth flotation flowchart.

Source: [99]

1.5 Current Practices and Recovery Methods

1.5.1 Hydrometallurgy Method

In hydrometallurgy processes, the leaching kinetic depends on varies leaching conditions, such as species of acids, the concentration of acids and reductants, reaction time, temperature and pulp density. Strong acids have strong ability to leach metals from LCO; Increasing the concentration of reductants such as hydrogen peroxide (H_2O_2)[21], sodium bisulfite ($NaHSO_3$)[68] and succinic acid[26] can enhance the reduction of Co(III) to Co(II),[102] which further improve the leaching efficiency. Recently, glucose is also being studied as a

reductant for increasing the efficiency in the leaching process due to its stability and low cost.[103]

As shown in **Figure 1.12**, ultrasonication is often used in hydrometallurgy method to induce high localized temperatures, pressure, and shear forces to improve metal leaching efficiency.[91, 92] For instance, cavitation effects and microbubble formation cause a series of physical and chemical changes to the structure of LCO cathode material, which enhanced the leaching efficiency of metals from spent LIBs while reducing the time.[4, 89, 90] Martínez proposed that around 86% of Co and Ni recovery efficiencies was achieved with the 40 KHz ultrasonication and 1.5 M citrate acid under a mild temperature (55^{o}C).[104] Jiang et al. also achieved 94% and 98% for Co and Li respectively by using 2 M H_2SO_4 and 360 W ultrasonic power at 30 minutes.[105] By contrast, the same hydrometallurgy process without ultrasonication, 20 more minutes of the reaction time or 30^{o}C higher of the temperature were needed to achieve same leaching efficiency.

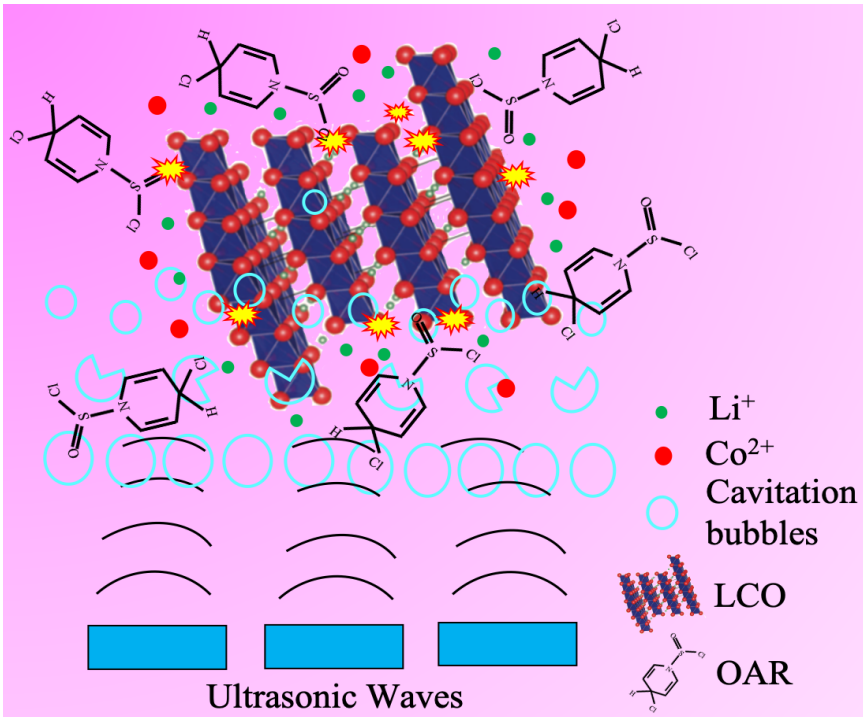

Figure 1.12 The schematic of a hydrometallurgical method with ultrasonication**.**

1.5.2 Pyrometallurgy Method

Pyrometallurgy, widely used by industries such as Umicore, Accurec, Sony, Onto and Inmetco,[106] involves the combustion of organic materials at high temperatures to reduce and smelt metals. **Figure 1.13** shows the spent batteries are first pyrolyzed in a furnace at 300-500 ºC to evaporate the electrolyte and plastic housing.[49] After this step, the pyrolyzed batteries are cooled down and re-melted in a second furnace with higher temperatures of 1400-1700 ºC where they are transformed to metal alloys.[49] However, Li is usually lost in the form of slag residue and gaseous Li_2O or Li_2CO_3 due to the high temperature (over 500 ºC). Thus, a hydrometallurgical process is combined with pyrometallurgy to recover the Li from LCO type of cathode materials. Thomas Tra¨ger et al.[107] reported a modified

pyrometallurgy with direct vacuum evaporation and selectively entraining gas evaporation at 1400-1650 ºC for 2 hours to recover Li from mixed types of cathode material. Zhang et al.[108] proposed a pyrolysis-enhanced flotation process to recover graphite and LCO at the temperature of 500ºC, which resulted in a recovery efficiency of 98%. Hu et al.[109] separated cathode materials from Al foil with 1.5 M NaOH, which was roasted 3 hours at a temperature of 650 ºC with addition of lignite (as a carbon source) to produce Li_2CO_3. 84.7% of Li and 99% of Co were ultimately recovered from the LCO type of cathode materials. Pyrometallurgy method has been commercially used to recover most of the current disposal LIBs, however, certain disadvantages including low efficiency, high energy consumption, involving risk and the secondary pollution are still existing and hampering the development of LIBs recovery.[110]

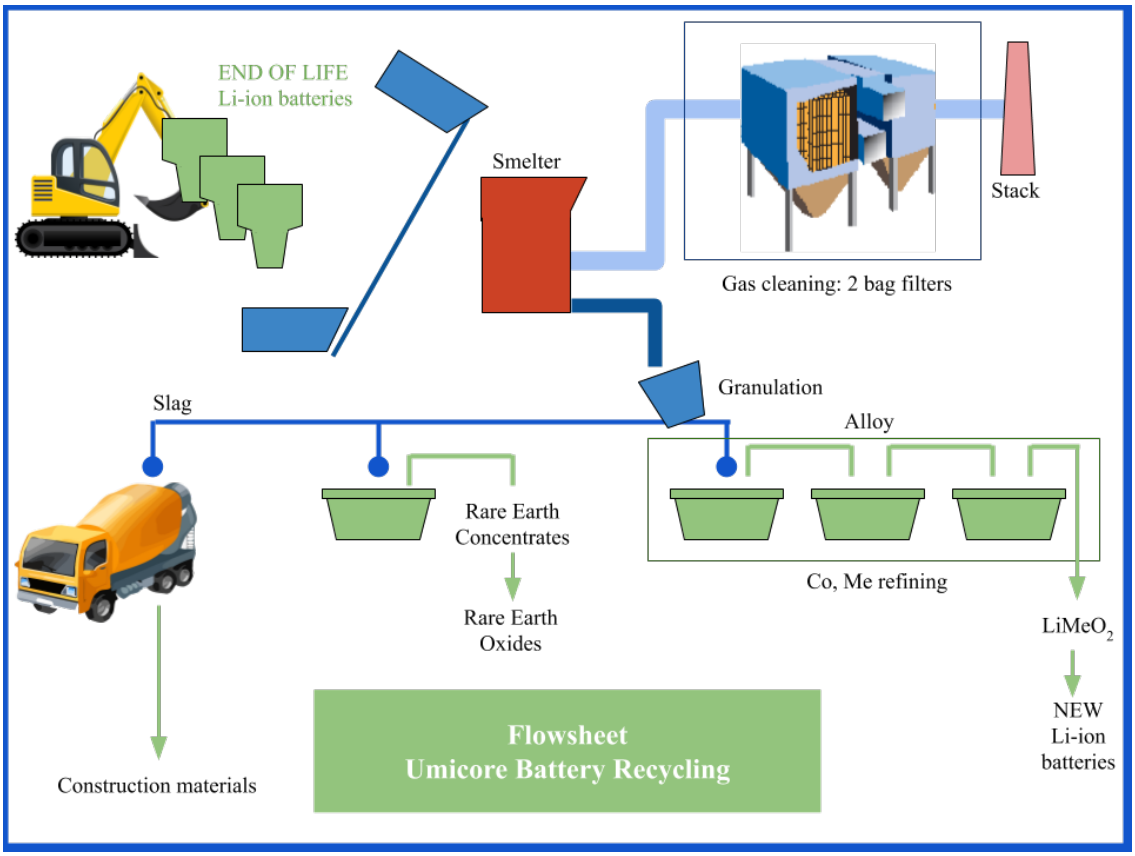

Figure 1.13 Schematic of pyro-metallurgy LIBs recycling process by Umicore™.

Source: [111]

1.5.3 Bioleaching Method

Bioleaching (Biohydrometallurgy) is gradually being accepted as an effective method of metal recovery that involves naturally-occurring, acidophilic iron and sulfur oxidizing microoganisms for the facilitation of metal dissolution processes due to its low energy and mild reaction conditions as shown in **Figure 1.14**.[112113-115] Bioleaching can be performed through the approach of one step and two step. In the one step, the LIBs powder and bacterial inocula are added immediately to the culture medium, whereas in the two step, the LIBs powder is added when the microorganism reached its maximum growth.[116] Mishra

et al. first reported bioleaching process with the iron and sulfur oxidizing bacterium, *Acidithiobacillus ferrooxidans*, which achieved 7 and 41% recovery efficiencies for Li and Co respectively under the leaching condition of 5 $g \cdot L^{-1}$pulp density, pH= 2.5, 1% elemental sulfur and 3 $g \cdot L^{-1}$ Fe(II) solution.[117] This microbe can produce a great number of reductants (e.g., Fe^{2+} and $S_2O_3^{2-}$) in the pyrite (FeS_2) bio-oxidation through the thiosulfate pathway,[118-120] which facilitates the dissolution of cathode materials of LIBs and performs the feasibility when recover Li and Co from spent LIBs.[121, 122]

Horeh et al. studied the application of fungal species, *Aspergillus niger,* on the recovery of mixed type cathode and anode materials from LIBs, obtaining 95 and 45 % for Li and Co recovery efficiencies respectively in the presence of citric, malic, gluconic and oxalic acid.[27] Niu. et al. utilized *Alicyclobacillus sp*., a sulfur-oxidizing bacteria (SOB) and *Sulfobacillus sp.,* an iron-oxidizing bacteria (IOB), for bioleaching process, which yielded the extraction efficiency of 89 and 72 % for Li and Co.[123] Ahmad Heydarian et al. investigated a mixed culture of chemolithoautotrophic mesophilic bacteria *A. thiooxidans(A.f)* and *A. ferrooxidans(A.t)* at a pulp density of 40 $g \cdot L^{-1}$ under optimized conditions (pH = 1.5; FeSO4 = 36.7 $g \cdot L^{-1}$; sulfur = 5.0 $g \cdot L^{-1}$), which yielded recovery efficiencies of 99.2 and 50.4% for Li and Co in the forms of $LiSO_{4(aq)}$ and $CoSO_{4(aq)}$.[113] Bioleaching for recovery valuable metals from spent-LIBs elicits low environment impact and low cost, but is usually time consuming with uncertainties in microbial cultures and their stablity.[27, 110] In addition, bioleaching offers a slow leaching efficiency when the mass

transfer is inactive, thus, an effectively bioleaching technology is necessary to study for the future application.

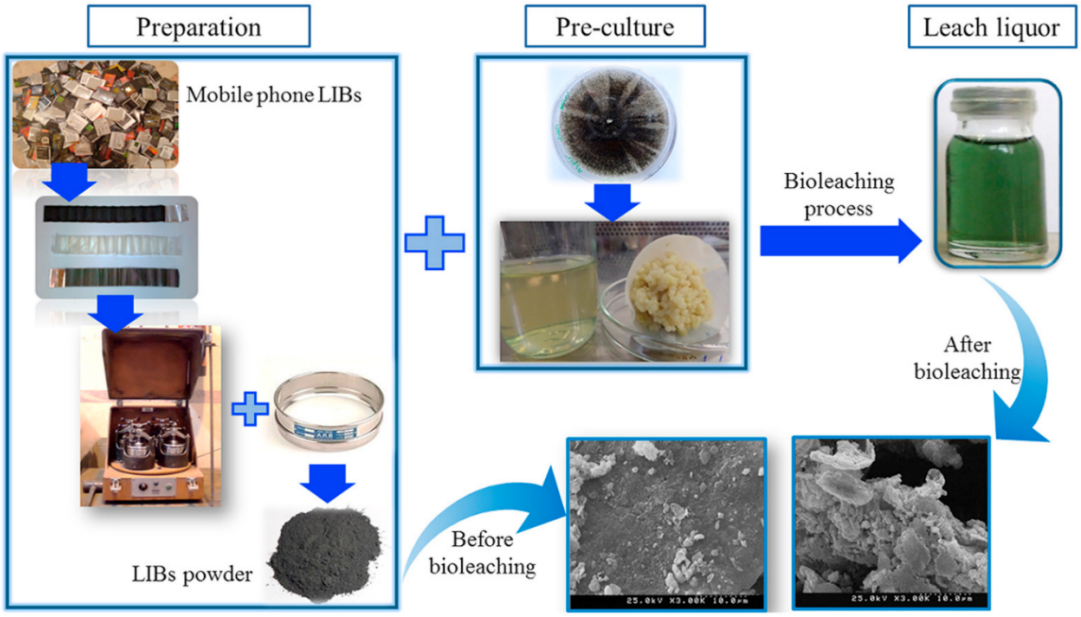

Figure 1.14 The schematic of bioleaching method using a bacteria species, *Aspergillus niger*.

Source:[124]

1.6 Applications of Organic Acids in Li/Co Recovery from Spent LIBs

1.6.1 Organic Acids: Principles and Applications

Many organic acids are increasingly used to dissolve cathode materials to recover Li/Co as they demonstrate equivalent or better leachability as inorganic acids but generate less toxic gases and secondary pollutants. Moreover, they could be produced naturally or with green chemistry. For example, citric acid is widely used leaching agent on the valuable metals recovery from spent-LIBs . Citric acid is a six-carbon tricarboxylic acid, which was first

isolated from the natural source, lemon juice. It is highly soluble in water as an excellent chelating agent which binds metals by making the metals soluble, and cheaper compared with other organic acids such as succinic acid, DL-malic acid and tartaric acid, as shown in **Table 1.6.** Golmohammadzadeh et al. recovered 92.53% and 81.50% of Li and Co from LCO respectively after 2 hours of immersion in 2 M citric acid at a pulp density of 30 g L^{-1} under 60 °C with 42mM H_2O_2.[16] Y. Fu et al. reported the highest recovery rates of 99.58% and 96.53% of Li and Co from LCO after 100 minutes using 0.75 M Benzenesulfonic acid at a pulp density of 15 g·L^{-1} under 90 °C with 100mM H_2O_2.[125] P. Ning et al. explored DL-malic acid for for the recovery of NMC type cathode materials and obtained the leaching efficiencies of the Ni, Co, Mn, and Li were 97.8%, 97.6%, 97.3%, and 98%, respectively after a leaching time of 30 min at a pulp density of 5 g L^{-1} under 80 °C with 140mM H_2O_2.[126] X. Chen et al. reported an over 98% and 97% leaching efficiencies for Li and Co respectively were achieved under the optimum leaching conditions of 0.6 M tartaric acid concentration, 100 mM H_2O_2, 30 g·L^{-1} pulp density and 80°C temperature for 30 minutes.[127] Musariri et al. indicated that the 95% and 97% leaching efficiencies of Li and Co were achieved at different concentrations of organic acids (1.5 M for citric acid and 1 M DL-malic acid) under the same conditions of other factors.[128] Generally, the concentration of citric acid has an effect on the leaching performance, with an increase in Li and Co leaching efficiency as the increasing concentration of citric acid from 1 to 1.5M. Nevertheless, this is not found in DL-malic acid.

The leaching kinetics has been described by different models including layer mass transfer control model, surface chemical reaction control model[26, 129], residue layer diffusion model[68, 75, 129] and Avrami equation[77]. Among these models, Avrami equation is originally developed for the kinetics of crystallization, in which each leaching condition is analyzed. In addition, Jha et al. investigated the leaching of Li and Co and focused on the determination of rate-limiting step and the corresponding activation energy, in which the leaching of Li and Co is controlled by either chemical reaction and diffusion through the ash respectively. [18] Zheng et al. reported the kinetic study of Co recovery from spent LIBs using citric acid at temperatures higher than 70 ^{o}C.[72] The results showed that leaching of Co is controlled by chemical reaction. Li et al further to found out that Co and Li recovery using succinic acid was controlled by chemical reaction from 0–10 min and controlled by diffusion reaction from 20–40 min,[26] which matched with the surface chemical reaction control and residue layer diffusion models respectively. A comparison of activation energy (Ea) from references were sorted out in **Table 1.7**.

Table 1.6 Comparison of the Hydrometallurgy on Leaching Performance for Valuable Metals from Spent-LIBs by Various Organic Acids

Ref.	Type of LIBs	Acid	Temp (°C)	Pulp density ($g \cdot L^{-1}$)	Time (hr)	Efficiency (%)
[24]	LCO	1.5 M Citric acid	90	30	2	Li:98, Co:96
[29]	LCO	1.5M DL-malic acid	90	20	0.67	Li:~100, Co:>90
[26]	LCO	1.5M Succinic acid	70	15	0.67	Li: >96, Co:~100
[76]	LCO	1.5M Oxalic acid	80	50	2	Li, Co: >98
[77]	LCO	1.25M Ascorbic acid	70	25	0.5	Li: >98, Co: >95
[13]	LCO	1.5M Aspartic acid	90	10	2	Li, Co: >60
[77]	NMC	1.5M TCA	60	50	0.5	Li: 99, Co: 92
[128]	LCO	1.5 DL-malic acid	95	20	0.5	Li: 97, Co: 95
[16]	LCO	2M Citric acid	60	30	2	Li: 92%, Co: 81%
[125]	LCO	0.75M Benzenesulfonic acid	90	15	1.67	Li: 99%, Co: 96%
[126]	NMC	1M DL-malic acid	80	5	0.5	Li: 98%, Co: 97%
[127]	LCO	1.5M Tartaric acid	80	30	0.5	Li: 98%, Co: 97%
[128]	LCO	0.5 M glycine+ 0.02M ascorbic acid	80		6	Co: 95%

Table 1.7 Comparison of Activation Energy (E_a)

Ref.		Chemical reaction				Diffusion reaction			
		Li		Co		Li		Co	
unit		E_a	R^2	E_a	R^2	E_a	R^2	E_a	R^2
		$kJ \cdot mol^{-1}$							
[28]	1.2M Malic acid	20.3	0.99	29.9	0.98	22.6	0.99	31.2	0.99
[129]	3.5M Acetic acid	41.3	0.99	41.2	0.98	52.04	0.96	54.22	0.96
[128]	1M Malic acid	--	--	45.9	0.98	--	--	54.6	0.98
[128]	1M Citric acid	--	--	41.4	0.99	--	--	50.88	0.99
[25]	1.5M Succinic acid	8.9	0.91	13.6	0.95	25.94	0.95	--	--
[67]	1M Sulfuric acid	--	--	--	--	20.1	0.99	26.8	0.99
[18]	2 M Sulfuric acid	32.4	0.97	59.8	0.98	32.4	0.97	59.8	0.98

1.6.2 Organic Aqua Regia (OAR): Principles and Applications

Aqua regia is a mixture of hydrochloric acid (HCl) and nitric acid (HNO3) at a specific ratio of 3:1, which is widely used in dissolving and recovering noble metals(Ag, Pd, Au and Pt) especially for Au, from Wasted Electric and Electronic Equipment (WEEE). Aqua

regia are able to dissolve noble metals because each of its two component acids acts as a different function. HNO_3 is a good oxidizing agent, and Cl^- from the HCl from coordination complexes with the gold ions, removing them from solution. However, the nonselectivity of the inorganic acids results in the dissolution of other noble metals such as Ag, Au, and Pd at the same time as Pt which limits the quality of the recycled Pt. To address this issue, in 2010, Lin et al. discovered a new "organicus liquor regius" or Organic Aqua Regia (OAR) made by combining pyridine (Py) with $SOCl_2$ (reagent grade, 97%) with the volume ratio of 3:1 (molar ratio of 4.1:1.2) in the cold water bath (5-10°C).[130] OAR is formed with the sulfur atom in $SOCl_2$ as an electron acceptor and the nitrogen (or phosphor) in Py as an electron donor, following this reaction: $C_5H_5N + SOCl_2 \rightarrow ClSONC_5H_5Cl$.[131] This mixture is shown to dissolve noble metals (e.g., Ag, Au and Pt) rapidly under mild conditions (25-40°C) due to the formation of donor-acceptor adducts between reagents.[132] Compared with inorganic chemistry, organic chemistry provides precise control over chemical reactivity, and the ability to tailor organic reactions enables the selective dissolution of noble metals.[131] Besides, the excess of $SOCl_2$ after dissolution can be simply removed by purging the solution with nitrogen gas, and dilute OAR is relative safe to use. Thus, there are many potential applications of OAR such as metallurgy, metal etching for integrated circuit fabrication in electronics and especially for the recovery of noble metals. **Figure 1.15** summarizes the various materials that were reported to dissolve in the $SOCl_2$/Py system with chemical structures for Py and potential structure for OAR.

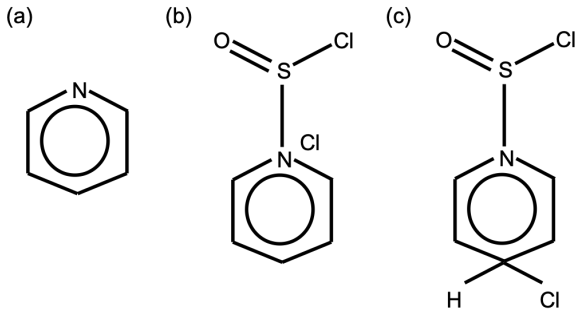

Metal	Dissolution (Y/N)
Ag	Y
Au	Y
Pt	N
Pd	Y
Cu	Y
Fe	Y
Ti	N
tungsten	N
tantalum	N
Cr	N
Sn	Y
In	Y
Teflon	N
Si	N
SiO_2	N

Figure 1.15 The chemical structure of (a) Py and potential structure for (b), (c) OAR and the reported materials that can be dissolved by OAR.

Source: [131]

1.7 Research Objective

The purpose of this study is to investigate an ultrasonication assisted leaching process with an novel leaching reagent, OAR, to chemically recover Li and Co from LCO type spent-LIBs. Besides, this study is aiming to simplify the recovering process and reducing the complicated and high energy consumption pretreatment process. OAR has demonstrated excellent chelating ability and potential to be reachable or reused like organic acids.[131] LCA analysis was further conducted to compare CO_2 emission potential from different hydrometallurgy processes using OAR, sulfuric acid and citric acid respectively to assist in understanding the environmental impacts and sustainable product or process design.

Therefore, the recovering process can be advanced beyond the laboratory scale to achieve industrial scale for spent-LIBs solid wastes.

CHAPTER 2

MATERIALS AND METHODS

2.1 Materials and Pretreatment

2.1.1 Reagents and Analytical Method

Nitric acid (TraceMetal^{TM} Grade) and hydrochloride acid (TraceMetal^{TM} Grade) were purchased from fisher scientific. Citric acid (ACS certified), thionyl chloride ($SOCl_2$) and Pyridine (Py) were purchased from Sigma Aldrich. Organicus liquor regius (OAR)[130] was prepared with mixtures of $SOCl_2$ and Py with the volume ratio of 3:1 in the cold water bath (5-10^{o}C). All the solutions were prepared using de-ionized water. Spent-commercial 18650 LIBs were taken from used laptop computers as shown in **Figure 2.1** All of the collected batteries were LCO type LIBs from different manufacturers as shown in **Figure 2.2.**

Figure 2.1 (a) Undergraduate students presenting a campus campaign poster for the EPA P2 project and (b) Undergraduate students involved in dismantling the LIBs in Dr. Zhang's laboratory. (c) Commercial 18650 cylindrical lithium ion batteries (LIBs) collected from used laptop, and the tools to dismantle the laptop battery cell.

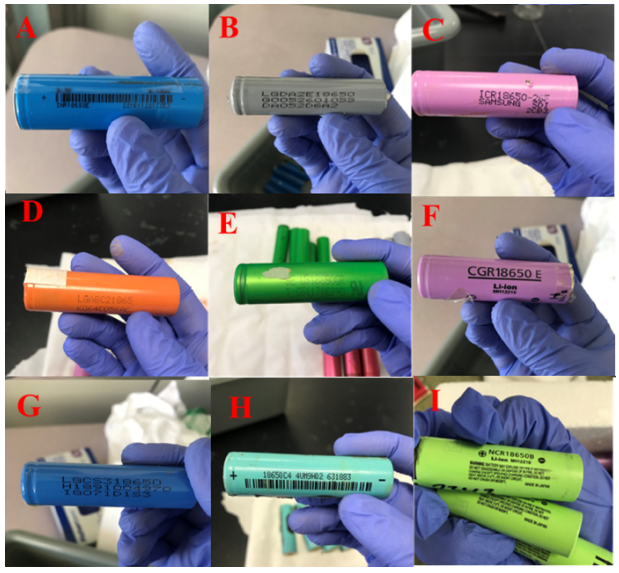

Figure 2.2 Various collected LIBs with different brands or models of Samsung, LG, Sony, Sanyo and Panasonic.

2.1.2 Pretreatment Process of Spent LIBs

To avoid short-circuiting and self-ignition, the collected LIBs were immersed into a 10 wt. % NaCl solution for 48 hours in a chemical fume hood to discharge completely. LIBs were then washed by de-ionized water to remove rusty materials from the surface and air dried for 24 hours as shown in **Figure 2.3.** The plastic and metal cases were manually removed

with sharp-nosed pilers in the fume hood. As shown in **Figure 2.4**, LIBs have layers structure where anode/separator/cathode/separator in a repeating sequence. The anode, metal case and separators can readily be recycled or reused.[133] Once uncurled and separated, the cathode material was dried at 60°C for 24 hours in crucibles in an oven to evaporize the electrolyte. The dried cathode material was cut into small pieces with scissors for characterization and leaching experiments.

Figure 2.3 Discharge process (a) LIBs in 10 wt. % NaCl solution; (b): after 48 hours discharge; (c) air dried LIBs after washed with DI water.

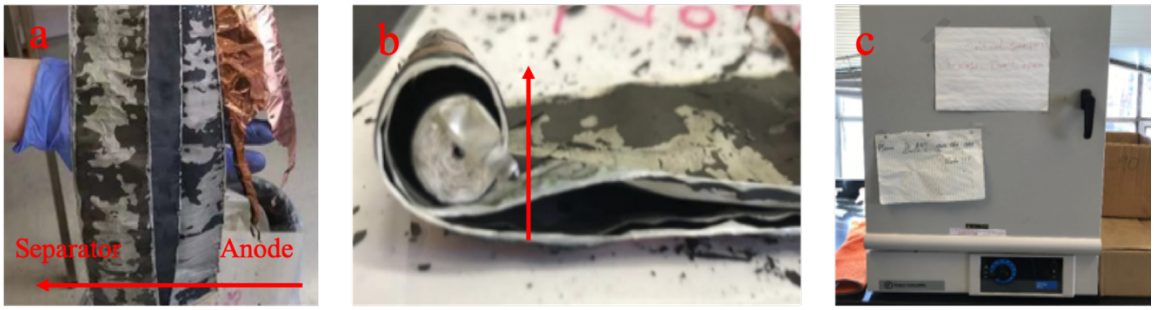

Figure 2.4 When opening the spent-LIBs, (a) and (b) inner structure is layer by layer rolling to a cylindrical shape. (c) the cathodes are dried at 60°C for 24 hours before leaching.

2.2 Characteristic Changes of Active Cathode Materials Before/After Leaching

The crystallinity of LCO powder and residue after leaching was analyzed by X-ray diffraction (XRD, Rigaku, RXIII) on a D/MAX-2500 unit with Cu Ka radiation (k = 1.54056 Å). Before the analysis, the samples were finely powdered in an agate mortar and then were scanned from 10° to 80° using 0.5° steps and a count time of 1 s.[26] A UV-visible spectrophotometer (EVOLUTION 201, Thermo) was used to detect chemical constituents such as cobalt complexes in the leaching solutions. The surface morphology of LCO powder and residue after leaching were examined by a Scanning Electron Microscopy (SEM; JSM-5610LV, JEOL, Tokyo, Japan) with energy dispersive spectroscopy (EDS). Briefly, the sample was prepared by sprinkling LCO powder onto a carbon conductive tab covered aluminum stub. The loose, excess powder was blown off with an air gun. The loose, excess powder was blown off with an air gun.), and then sputter coated with 8-nm thick gold under vacuum. The SEM images were taken at various magnifications and sample locations. The specific surface area of the LCO powder is determined by Brunauer-Emmett-Teller (BET) N_2 adsorption in the relative pressure range of $0.05 \leq (p/p_0) \leq 0.30$ using an Autosorb iQ apparatus (Quantachrome Autosorb iQ-MP, Automated Gas Sorption Analyzer).[134] Prior to the measurement, all samples were degassed under dynamic vacuum at 200°C for 12 hours at a rate of 10 °C·min^{-1} under vacuum.

2.3 Quality Control/ Quality Assurance

2.3.1 Data Quality and Reporting Limits

For ICP-MS analysis, several verification checks were performed after Initial Calibration Blank Validation (ICBV) and Initial Calibration Validation (ICV) every 15-20 samples and at the end of analysis. The proficiency of the ICP-MS analysis was determined by the observation of their QA/QC performance. This includes factors such as: stable spectra or any spectral interferences, the relative standard deviation (RSD) on replicates of unknown or repeatability of sample results with known concentrations.

a. Precision: The precision of the analysis was examined using the relative percent different of duplicate samples, RSD, which is calculated by **Eq. 2.1.**[135]

$$RSD=100[\frac{(X1-X2)}{X1}] \quad (2.1)$$

where X1 = First observation of sample result, X2 = Second observation of sample result and RSD values of 15% will be acceptable. If RSD > 15%, samples will be reanalyzed with adjustments such as sample pretreatment, purification, dilution or instrumental maintenances if needed.

b. Accuracy: The accuracy of the measurements will be tested with a Continuing Calibration Verification (CCV) every 15-20 samples. In addition, blind standards run as samples with known concentrations were placed between samples as a secondary quality

control check for accuracy. We will consider the instrument is out of accuracy when the measured value is deviated of the standard deviation more than 20%.

c. Representativeness: Each experiment had a specific sampling protocol prior to conducting any sampling, which were reviewed by the QA officer (i.e., faculty advisor), with the objective of ensuring the representativeness of the samples. The number of the collected sample and the sampling strategy will depend on the specific experiment duration and objective. Representativeness within the sample will be achieved by homogenization of each sample through thorough mixing before the analyses.

d. Comparability: Comparability of the data was obtained by following the same operational procedure for sample collection, processing and analysis.

e. Completeness*:* It is the responsibility of the project to ensure that: (1) all the samples required per the sampling protocol are collected; (2) that the samples are properly labeled and preserved; (3) that all the quality control checks are included; (4) that all the information required for sample preservation and preparation is completed; (5) that the samples are analyzed and the results are received within a reasonable amount of time; (6) that the analysis has passed all the quality control checks within 20% of error; (7) that if there is any problems with the analysis is recorded and communicated; (9) that the results generated from the analysis are stored and saved

2.3.2 Instrument Calibration and Frequency

Inductively Coupled Plasma-Mass Spectrometry (ICP-MS, Agilent 7700, the USA), as shown in **Figure 2.5,** was calibrated prior to any analysis. The calibration curves had at least 5 points plus a blank in the curve, ranging from the lowest to the highest expected concentrations of the samples to be analyzed (based on historical knowledge of the area, research estimation). The calibration curves for Li and Co were obtained using the standard solutions of Li and Co (1000 ppm) to dilute into 8 different levels (1 ppb to 200 ppb) using 2% (0.3 M) nitric acid. If the method requires validation (for new methods or high-priority samples), another calibration curve (standards as samples) may be repeated at the end of the analysis, for other measurements such as pH and conductivity, instruments are calibrated according to manufacturer's instructions. In general, the calibration will be accepted if the squared correlation coefficient (R^2) is > 0.99.

According to the molecular formula of LCO ($LiCoO_2$), the mass of Co accounted for approximately 59% and Li accounted for 7%, respectively. Since 10 grams of LCO powders were immersed in the leachant solution (333 mL of the OAR solution and 25 ml of H_2O_2), the maximum concentration for Co and Li, if fully dissolved, would be 16 and 1.9 ppm, respectively. In the ICP-MS, the leachant samples were diluted for at least 10^5 times to achieve sensitive detection by the ICP-MS.

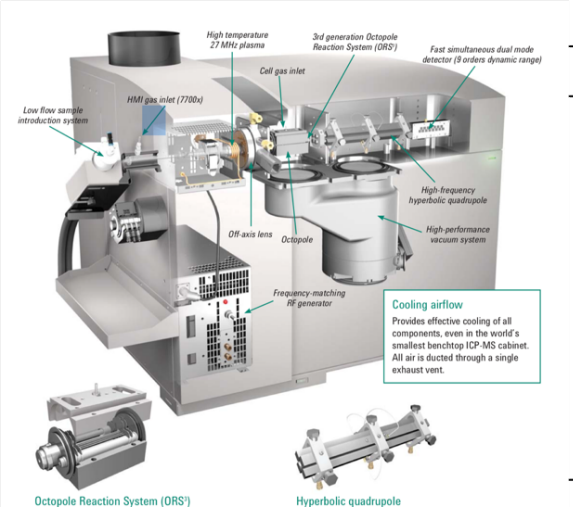

Parameters	Values
RF power (W)	1000
Plasma argon ($L \cdot min^{-1}$)	15
Nebulizer flow ($L \cdot min^{-1}$)	0.9-1
Nebulizer	Cross-flow
Resolution	Normal
Dwell time (ms)	50
Number of replicates	3

Figure 2.5 The components and operation parameters of the ICP-MS.

2.4 Leaching Efficiency and Kinetics Study

2.4.1 Leaching Efficiency Study for OAR and other Acids

2.4.1.1 Organic Aqua Regia (OAR)

Figure 2.6 shows the schematics of OAR preparation, including three major steps: discharging and dismantle, leaching and analysis. The leaching experiments are carried out in 1000-mL PP bottles under 120-W ultrasonication (Fisher Scientific Sonic Dismembrator Model 500) as shown in **Figure 2.7**. The leaching experiments were conducted with various OAR concentration (0.015, 0.09, 0.03, and 150 $\mu g \cdot mL^{-1}$), temperature (45, 55, and 65 ^{o}C), pulp density (30, 40, and 50 $g \cdot L^{-1}$), reaction time (0- 70 minutes) and H_2O_2 (0, 1, 3, and 4% v/v). The leaching solution was vacuum filtered by Whatman filters (0.45 µm, 47 mm in diameter) to remove the insoluble residue. A wine-red filtrate was obtained and then fully digested in Aqua Regia (1-mL Aqua regia: 10-mL filtrate) and filtered with the

Whatman membrane filter again before the ICP-MS analysis for the concentration determination of Co and Li. The concentrations of the recovered Li and Co were further used to calculate the leaching efficiency by **Eq. (2.2).**

$$E(\%) = \frac{C_1 \times D}{(M_1 - M_2) \times M_3 \times W_1} \times 100\% \qquad (2.2)$$

where E(%) is the leaching efficiency, C_1 is the concentration result directly reported from the ICP-MS, D is the dilution factor or dilution times, M_1(g) is the initial mass of the cathode sample, M_2 (g) is the mass of residue after filtration, M_3 (%) is the percent of the metal of the total mass number in the LCO cathode material, W_1(ml) is the weight of the leachant (leaching acid and reducing agent) with assumption that the density of leachant is close to water.

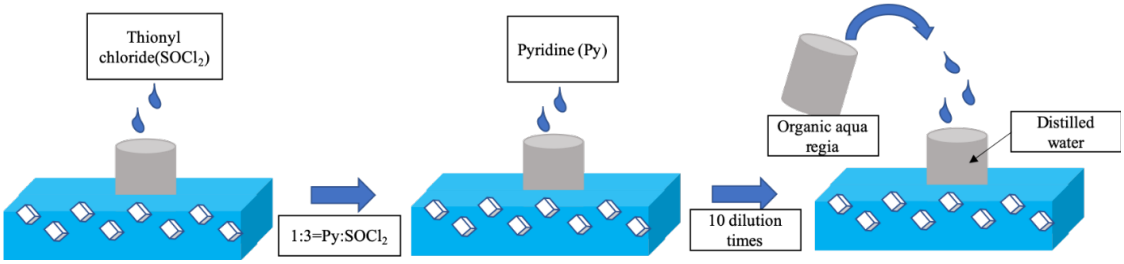

Figure 2.6 The process when preparing and diluting the OAR in an ice water bath.

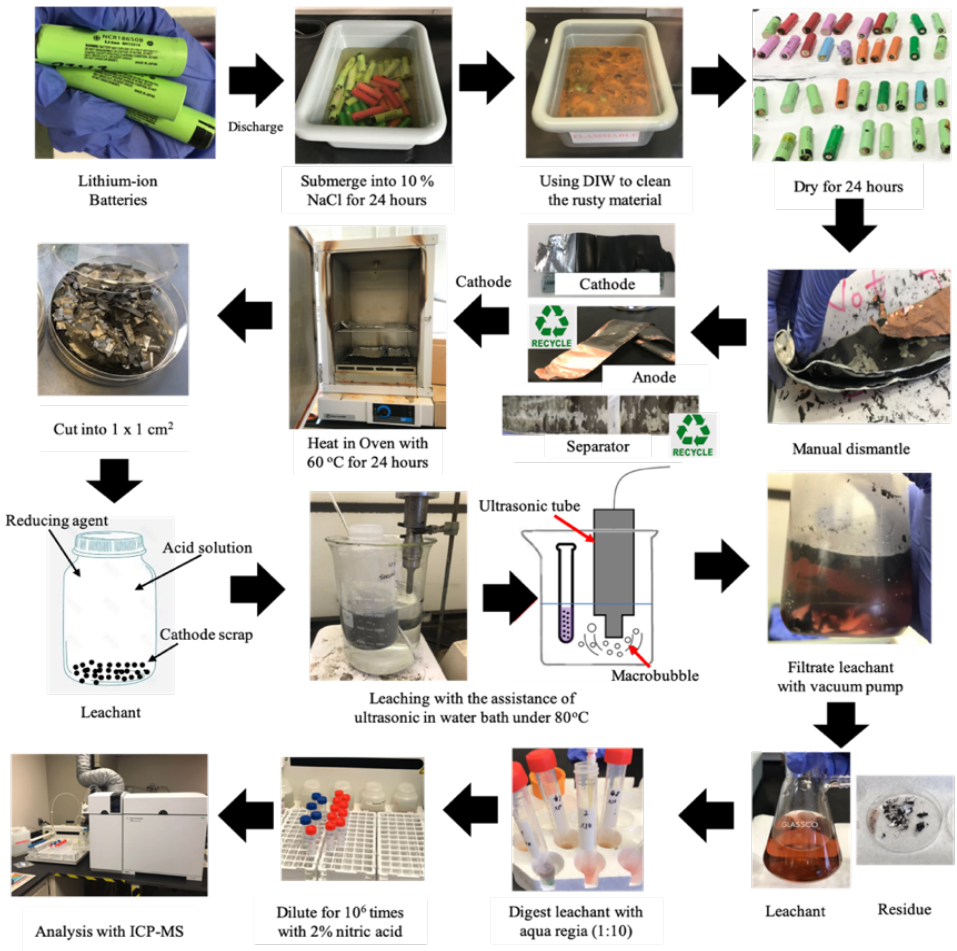

Figure 2.7 The schematic of hydrometallurgy processes (e.g., spent LIB discharge, separation of cathode and anode, leaching experiment and analysis of leachant with ICP-MS).

2.4.1.2 Citric Acid and Nitric Acid

Citric and nitric acids are two widely used leaching reagents on the valuable metals recovery from spent-LIBs which are used here as the representatives of organic and inorganic acid for the comparison purpose. By compare the leaching efficiencies of OAR, the same experiments were carried out with 1 M citric acid or nitric acid at a pulp density of 30 $g \cdot L^{-1}$ with 100 mM H_2O_2 under 65 °C and 120-W ultrasonication for 60 minutes.

2.4.2 Dissolution Kinetic Study and Release Rate Determination

Dissolution rate study was conducted to determine the leaching kinetics of Li and Co at different solution temperatures (45, 55, and 65 °C) for leaching times (0-60 minutes). Other conditions remained the same as those described above (e.g., 100 mM H_2O_2, 148 mg·mL^{-1} OAR, and a pulp density of 30 g·L^{-1}). The leaching of LCO is a heterogeneous reaction and is mainly controlled by either chemical reaction or diffusion.[28, 75, 136] The leaching reaction process is described as **Eq. (2.3)**[26, 129] when leaching is controlled by chemical reactions, and is described with **Eq. (2.4)** when leaching is controlled by the diffusion through the boundary layer according to the shrinking-core model for the leaching kinetics of shrinking particles.[26, 28] The relationship between dissolution reaction rate constant and temperature can be further described by the empirical Arrhenius law as **Eq. (2.5)**.

$$k_c t = 1-(1-x)^{\frac{1}{3}} \tag{2.3}$$

$$k_d t = 1-\frac{2}{3}x-(1-x)^{\frac{2}{3}} \tag{2.4}$$

$$k = Ae^{\frac{-E_a}{RT}} \tag{2.5}$$

where x is the leaching efficiency (%); k_c is the rate constant of chemical reaction (min^{-1}); k_d is the apparent diffusion constant (min^{-1}); t is the leaching time (min); R is the universal gas constant (8.314472 J·mol^{-1}K^{-1}); A is the pre-exponential factor (1·min^{-1}); E_a is the apparent activation energy (J·mol^{-1}), and T(K) is the absolute temperature.

The average release rate for Li and Co are calculated from **Eq. (2.6):**

$$v = \frac{C \cdot V}{M \cdot t} \tag{2.6}$$

where v is the leaching release rate; C is the equilibrium concentration of Li or Co ($mg \cdot L^{-1}$) in the leachant; V is the volume of the leachant (L); and M is the weight of the LCO scraps (mg).

2.5 Life Cycle Assessment of Li and Co Recovery from Spent-LIBs

2.5.1 Introduction to Life Cycle Assessment

Life cycle assessment (LCA) is an environmental accounting and management technique that considers potential environmental benefits of a product and pollution releases associated with an industrial system from cradle to grave.[137, 138] LCA can assist in identifying opportunities to improve the environmental aspect, product or process design and marketing as outlined in **Figure 2.8**.[138] Conventionally, the concept of a product's life cycle starts from its cradle, where raw materials are extracted from natural resource, through refinement, production, use then to its grave or end-life disposal.[139] To start LCA, the goal and scope shall be defined clearly and consistent with the intended application. **Figure 2.8** also illustrates the components of LCA including goal, scope, inventory analysis and interpretation of results. Life cycle inventory (LCI), for instance, includes compiling an inventory of environmentally relevant inputs and outputs related to the functionality of product.

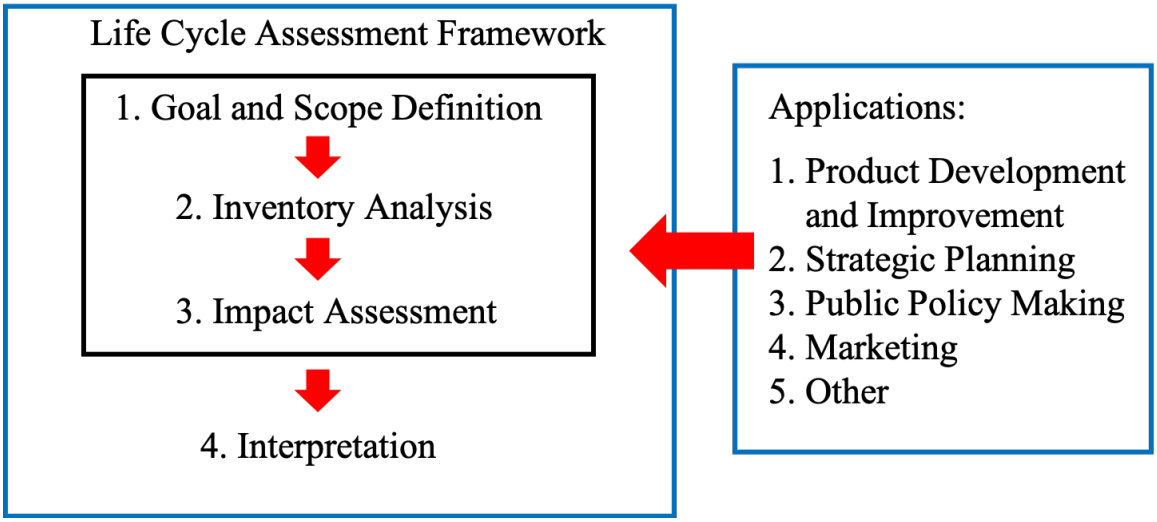

Figure 2.8 The framework and component of LCA.

2.5.2 Goal and Scope Definition

In this work, a process-based LCA after end-of-use of current commercial pyrometallurgy recovery technology, large-scale hydrometallurgy processes with citric acid and sulfuric acid, and the self-report lab-scale hydrometallurgy process with OAR for spent LIBs (LCO type of cathode material) was conducted. The goal of the investigation is to assess the CO_2 emissions from different recovery processes of Li and Co from spent LCO cathode cells. We assessed the major recovery processes including collection (transportation), pretreatment (discharge and dismantle), heating and recovery processes (hydrometallurgy) as shown in **Figure 2.9.** Functional unit (F.U.) is chosen as the collection, pretreatment and recovery of 1 ton of LCO cathode cell. Accordingly, the LCI of environmental impacts are evaluated based on this F.U.

Scenarios Description:

The LCA was carried out for hydrometallurgy method with OAR from our self-report process, and compared with the existing pyrometallurgy method and hydrometallurgy method with sulfuric acid and citric acid from GREET2 (2019 version), Argonne National Laboratory[140] for the potential recovery process development in industrial scale. The system boundary and the unit function are defined to be modelled by the study. The process flow diagram with the unit processes and the interrelationships where the unit processes start in terms of input of raw materials or intermediate products then the operations and transformations that occurs during the unit process and ends with destination of the intermediate or final products.[141]

Collection Points:

The collection points of the spent LIBs from portable electronics including commercialized lithium-ion recycling companies where people can request specific recycling kits (U.S. DOT special permit) then send back to companies such as Call2Recycle and Earth911 or counties recycling centers, especially in NJ, where people can find the related sites in Recycling NJ web.[142] The following retailers also have signed up to the batteries recycling scheme where spent-LIBs can be recycled from the people in these stores, such as AT&T, Best Buy, Home Depot, Staples, Sears, Target, Verizon Wireless, Black & Decker, DeWalt, Interstate All Battery Centers, Lowe's, Milwaukee Electrical Tool, Office Depot, Orchard Supply, Porter Cable Service Centers, RadioShack, Remington Product Company and US Cellular.[143] Disposing LIBs on neither these sites are considered as improper disposal

which will ended up in the landfill or incineration later. For the drop-off locations, a claim reports 87% of people living in the U.S. can recycle the batteries within 10 miles from the recycler,[144] thus, we are assuming the collection of batteries take 0.1miles to 10 miles per 50 pounds (no more than 66 pounds batteries can be shipped in the box according to the U.S. DOT regulations), with 5 miles per 50 pounds in average.

Transportation to Recovery Industrial Factory:

The LIBs after collection will be shipped to the recycling factory, Recycling Coordinator, Inc., which is located in Akron, OH and was funded in 1992. Currently, this is only one large-scale commercialized LIBs recycling factory has the cooperation with Call2Recycle in United States. We assuming that LIBs collected in the NJ will be shipped to here in priority in order to reduce the energy consumption from the transportation. Due to the complicated distribution of the collection centers and the chosen commercial trucks for shipping, the data be provided here are distance according to the google Map. The longest distance is 491, shortest distance is 391 mile and 441 mile in average from New Jersey several ancillary collection centers to recycling factory in Akron, OH with average carry capacity between 13,000 to 28,000 pounds per commercial truck according to the regulation of National Highway Traffic Safety Administration.[145] A more precise carry capacity for trucks mostly depend on the axles, truck size and weight limit laws.

Discharge and Dismantle:

As describing previously in this research, the process of discharging is to submerge around 1-kg LIBs into 2-L 10% NaCl solution for 48 hours without any heating equipment. After 48 hours, cleaning the LIBs with 2-L water to remove the robust and dirt. Normally, the dismantle process is crushing then sieving by means of several screens, and spent LIBs have above average selective crushing properties to accomplish the desired separation of components. In our lab-scale self-report process, we used the cutting machine to cut off the cap of LIBs and rip out the metal case with pliers, manually separating one LIB to one LCO cathode cell. It takes around 5-10 minutes to dismantle one LIB to one LCO cathode cell. The collected LCO cathode cells were sent into oven for vaporizing the organic solvent and electrolyte under 60 ^{o}C for 12 hours.

Hydrometallurgy Recovery Process with OAR:

Hydrometallurgy recovery process have the highest potential for industrial and commercialized scale. In comparison with this, pyrometallurgy is a kiln firing process following with leaching to recover slag and valuable metals.[14] The collected battery scraps are directly put into the smelter without pretreatment, aim at providing a closed-loop recovery of Co and Ni to resynthesize LCO. Li and Al are lost during the melting, carbon is burned and used as reducing agents for some of the metals.[36, 61, 111] To reduce the emissions, energy consumption and Li-lost problems during pyrometallurgy processes, more and more companies focused on the study of hydrometallurgy processes. Hydrometallurgy is chemical behavior with acid leaching process used to separate and

refine materials with the ability of exchanging both Co and Li.[14] This process can be further categorized into organic acid based (mostly citric acid) and inorganic acid based (mostly sulfuric acid and nitric acid). OAR based hydrometallurgy process combining with ultrasonication (120W, 20 kHz) has comparable potentials with sulfuric and citric acid based hydrometallurgical recovery processes due to the reduction of complicated pretreatment process, lower temperature and strong chelating ability.

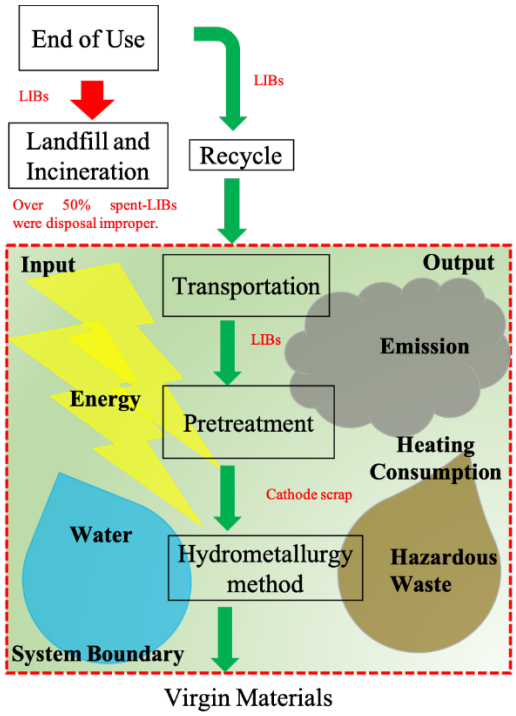

Figure 2.9 Study scope for battery collection and recovering process.

2.5.3 Framework of Life Cycle Inventory

Inventory Analysis:

Life cycle inventory (LCI) is a step to determine the mass flows, i.e. the raw materials, water, energy and emission releases to air, water and land and waste outputs associated

within the system boundary. The LCI was chosen as environmental analytical tool, include raw materials, electricity, emissions, transportation and recovering process. The contribution of this study is to quantify these benefits for LCO type LIBs recovery technologies with static modeling.

Impact Assessment and Interpretation:

To evaluate the life cycle impacts of hydrometallurgy method with OAR, LCIA results were obtained from corresponding environmental impacts with different emission categories according to the provided data from Material Safety Data Sheets (MSDS) and database from Argonne National Laboratory. The impact assessment may include elements such as assigning of inventory data to emission categories, modelling of the inventory data and possibly aggregating the results in specific and meaningful cases which provides the information for the LCI interpretation.[138] LCIA is different from other environmental impact assessment or evaluation techniques as it is a relative way based on a functional unit.[141] The interpretation is comprised with the evaluation of impact assessment results and a sensitivity analysis including assumptions, limitations and data quality assessment.

2.6 Statistical Analysis

The presented results are the mean values ± standard deviation (SD) from three independent experiments: (1) Leaching Efficiency; (2) Dissolution Kinetic Study and (3) Leaching Release Rate. The significant differences in the dissolution kinetic study and

leaching experiments under different factors were analyzed using variance analysis (ANOVA) at a significant level of p= 0.05. SEM images in **Figure 3.2** are typical results selected from at least 5 different sample locations. The minimum, mean and maximum values of emission for each process of LCA are calculated and estimated from MSDS and power range from the instrument manual.

CHAPTER 3

RESULTS AND DISCUSSIONS

Work of this chapter is related to or has been published through following manuscript or presetations:

Leqi Lin, Wen Zhang, 2020 Leaching of valuable metals from spent-lithium-ion batteries (LIBs) using Organic Aqua Regia, Resources, Conservation and Recycling. (Paper under preparation)*

Leqi, Lin, Wen Zhang, Leaching of valuable metals from spent-lithium-ion batteries (LIBs) using Organic Aqua Regia, ACS American Chemical Society 259th National Meeting, Pennsylvania Philadelphia, March 23th, 2020.

Leqi, Lin, Wen Zhang, Leaching of valuable metals from Lithium-ion batteries (LIBs) using green organic acids, Graduate Student Research Day, New Jersey Institute of Technology, NJ, 2019.

Leqi, Lin, Wen Zhang, Leaching of valuable metals from Lithium-ion batteries (LIBs) using green organic acids, EAS The Eastern Analytical Symposium and Exposition, Princeton, NJ, Oct 15th, 2019.

Leqi, Lin, Wen Zhang, Green chemical process to recovery Li and Co from spent Lithium-ion batteries, WEA NJ annual conference student poster contest, Atlantic City, May 7th, 2019.

3.1 Characteristic Changes of Active Cathode Materials Before/After Leaching

3.1.1 Crystallinity Analysis

XRD is a characterization technique for the crystalline structure, lattice parameters, planar spacing and crystalline size. **Figure 3.1** compares the XRD patterns for LIBs before and after acid leaching processes. The spectral peaks at (003), (101), (104) as well as weak peaks at (015), (017) and (018) indicate the presence of crystalline phases of LCO. Other weak peaks (006), (012), (110) and (113) are characteristic peaks for the impurities (e.g. CoO and C).[23, 24, 71, 73] After leaching, the intensities of all the peaks become weaker,

suggesting the leachant (OAR and H_2O_2) disrupted the crystallinity of LCO, which was also observed in a previous study using formic acid as leachant.[146]

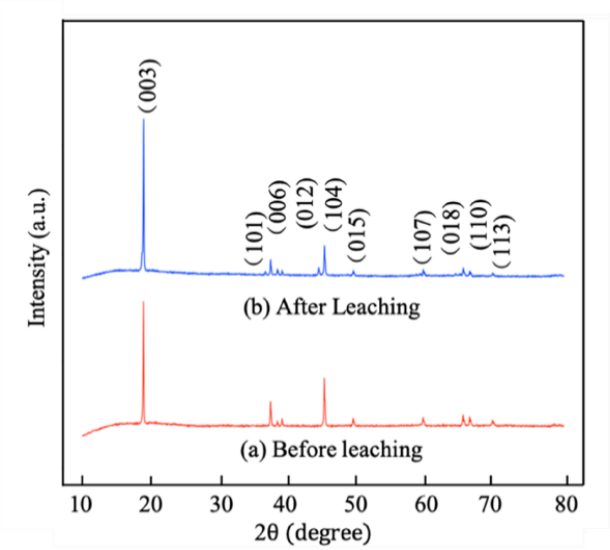

Figure 3.1 XRD patterns of (a) the raw material of LCO before leaching and (b) the cathode residue after leaching for 60 minutes by OAR acid with the following conditions [OAR]= 148 mg·mL^{-1}, temperature=65°C, [H_2O_2] = 100 mM, pulp density = 30 g·L^{-1} and ultrasonication= 120 W.

3.1.2 Morphological and Chemical Mapping

SEM images illustrate the morphological changes of LCO during acid leaching from 0-60 minutes. **Figure 3.2a** indicates the LCO particles had the element distribution of 3%, 62% and 17% for C, Co and O respectively. Due to the low atomic weight, Li element is out of the detected range under current SEM-EDS system. **Figure 3.2b-d** reveals that lamellar crystals of LCO particles have a diameter of 8.5 ± 3.5 μm, which is consistent with other literature.[23] After 20 and 60-minutes of leaching, the significant changes in particle shape and size indicate the dissolution of Li and Co by OAR. Similar observations of morphological changes were obtained with other acids such as nitrate and citric acids.

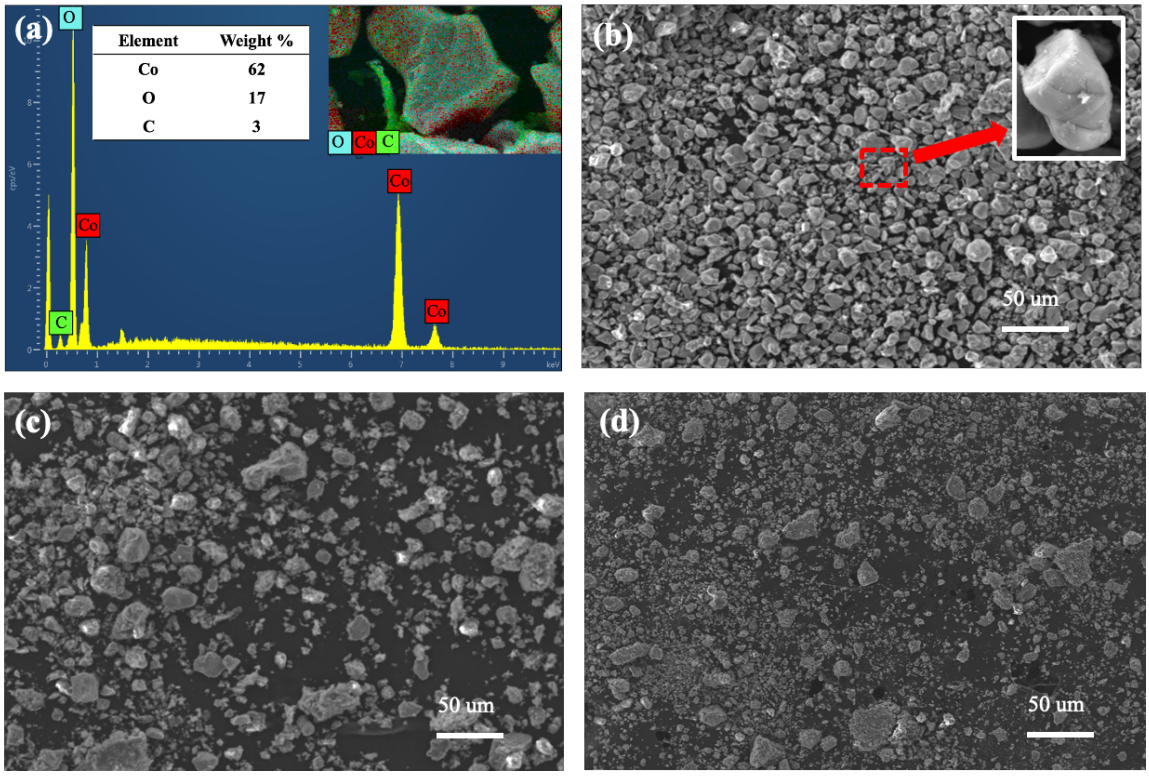

Figure 3.2 Morphological and chemical mapping by SEM-EDS (a) element distribution and mapping of elements from active cathode materials (LCO). SEM figures show the difference of LCO particles (b) before leaching (c) after 20 minutes and (d) after 60 minutes of the leaching process.

3.1.3 Leaching Mechanism with UV-Visible

Figure 3.3a demonstrates the UV-Visible spectra of the leaching solution from 20 to 100 minutes using OAR as leachant under conditions specified in the caption. The absorbance peak at around 290 nm is ascribed to the formation of Co(II) complex. There is a relatively weak absorbance peak at around 500 nm that is ascribed to the d-d transition in the Co(III) complex.[71, 73] The absorbance intensity at 290 nm increased with the increasing time, which indicates the reducing agent (H_2O_2) effectively reduced Co(III) to Co(II). The absorbance around 500 nm also slightly increased with time due to the concentration increase of the

leached Co(III). **Figure 3.3b** compares the absorbance peaks for the leaching solutions using three different acids after 60 min. The absorbance peak for OAR was higher than those of nitric and citric acid, suggesting that OAR yielded a higher leaching efficiency under the same leaching conditions.

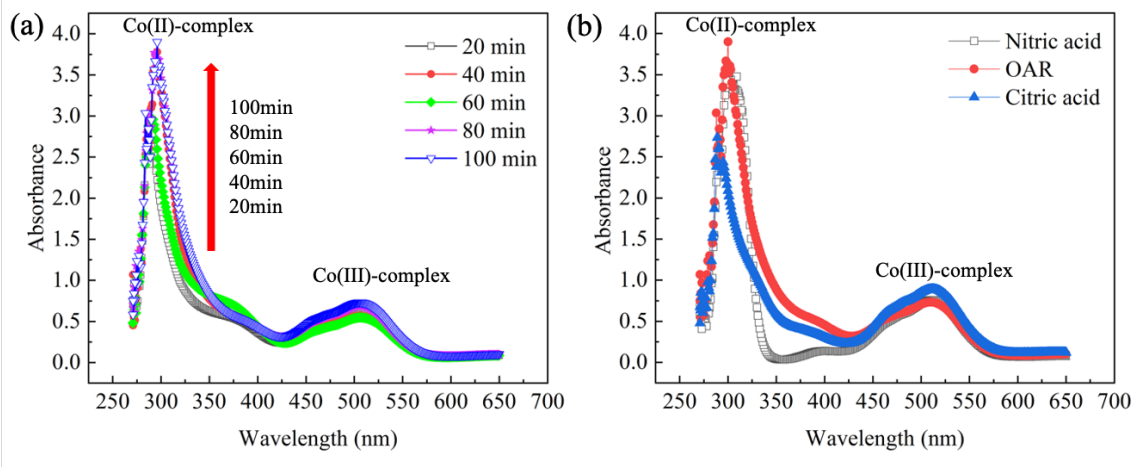

Figure 3.3. UV-visible spectra of the leaching solutions. (a) The absorbance peaks for the leaching solutions using OAR as leachant under the leaching condition (OAR: 148 mg·mL^{-1}, 100 mM, 65°C and a pulp density of 30 g·L^{-1}). (b) UV-visible results of three leachant proved that OAR has better ability than the other two acids.

3.2 ICP-MS Analysis

Figure 3.4 shows the calibration curves of Li and Co with the squared correlation coefficients (R^2) over 0.99. The RSD was 5% or less. The limits of detection (LOD) for Li and Co were 1.2 µg L^{-1} and 0.38 µg L^{-1}, respectively, which was estimated by depending on the system sensitivity using the following equation**:**

$$\mathrm{LOD} = \frac{S_b \times k}{m} \qquad \textbf{(3.1)}$$

where k is a factor with the value of 3, S_b is the standard deviation of the blank and m is the slope of the calibration graph in the linear range.

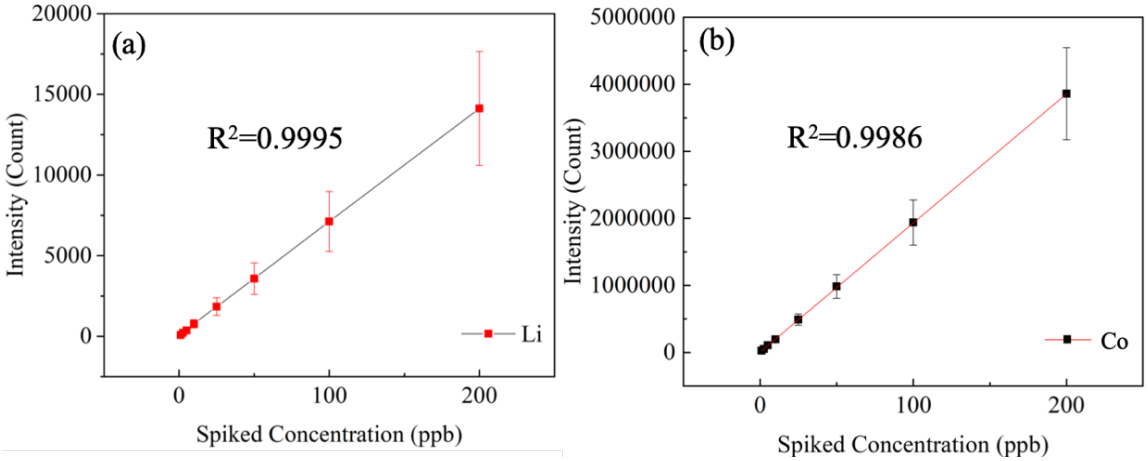

Figure 3.4 Calibration curves for (a) Li and (b) Co established with ICP-MS.

3.3 Leaching Efficiency Kinetics

3.3.1 Leaching Efficiency Comparison for OAR, Citric and Nitric Acid

Table 3.1 compares the reported leaching efficiencies for various LIBs using different organic acids as leachants. The common leaching temperatures are 60-95°C with pulp densities of 5-30 $g \cdot L^{-1}$ and leaching times of 0.5-6 h. As discussed above, high leaching temperatures promote more H^+ presenting in the solutions from the acid and accelerate the leaching reaction rate. Pulp densities affect leaching behavior as high pulp density means less leachant input to the LCO particle which is not sufficient to leach the LCO particle. This may attribute to low leaching efficiency. Clearly, the different organic acids achieved similar levels of leaching efficiencies of Li and Co over 90%. Some organic acids were claimed to be recoverable and reused for additional leaching processes. For example, citric

acid was regenerated by 0.5 M oxalic acid ($H_2C_2O_4$) and 0.5 M phosphoric acid (H_3PO_4), and was reused successfully without compromise in the leaching efficiency for 5 cycles.[24, 147]

Table 3.1 Comparison of the Hydrometallurgy on Leaching Performance for Valuable Metals from Spent-LIBs by Various Organic Acids

Ref.	Type of LIBs	Organic Acids	H_2O_2 (mM)	Temp (°C)	Pulp density ($g \cdot L^{-1}$)	Time (hr)	Efficiency (%)
This study	LCO	148 $mg \cdot mL^{-1}$ OAR	140	65	30	1	Li:99, Co:94
[24]	LCO	1.5 M Citric acid	10	90	30	2	Li:98, Co:96
[29]	LCO	1.5 M DL-malic acid	67	90	20	0.67	Li:~100, Co:>90
[26]	LCO	1.5 M Succinic acid	140	70	15	0.67	Li: >96, Co:~100
[76]	LCO	1.5 M Oxalic acid	500	80	50	2	Li, Co: >98
[77]	LCO	1.25 M Ascorbic acid	140	70	25	0.5	Li: >98, Co: >95
[77]	NMC	1.5 M TCA	140	60	50	0.5	Li: 99, Co: 92
[128]	LCO	1.5 DL-malic acid	57	95	20	0.5	Li: 97, Co: 95
[16]	LCO	2 M Citric acid	42	60	30	2	Li: 92%, Co: 81%
[125]	LCO	0.75 M Benzenesulfonic acid	100	90	15	1.67	Li: 99%, Co: 96%
[126]	NMC	1 M DL-malic acid	140	80	5	0.5	Li: 98%, Co: 97%
[127]	LCO	1.5 M Tartaric acid	100	80	30	0.5	Li: 98%, Co: 97%
[128]	LCO	0.5 M glycine+ 0.02 M ascorbic acid	67	80	--	6	Co: 95%

We evaluated the leaching efficiency using OAR (148 $mg \cdot mL^{-1}$) as a leachant under the condition of a $g \cdot L^{-1}$ pulp density, 65°C, 100 mM H_2O_2 and 120 W ultrasonication. **Figure 3.5a.** For the first 10 minutes, the efficiency is only 80% for Li and 62% for Co,

after that, an increase of efficiency to 99% for Li and 86% for Co when the time gets to 60 minutes. In order to leach Co from $(CoO_2)^-$, a reducing agent (H_2O_2) is necessary during the process, thus, for the first 10 minutes, Co has a low dissolubility then increases dramatically after 10 minutes. Co also has a relative slow leaching progress than Li during 10 minutes to 50 minutes, which may be caused by the diffusion reaction for the leachant reacting with residue surface. At 60 minutes, almost 99% for Li and 86% for Co which represent a proper leaching time for the next experimental approach and study.

The leaching process for both metals is usually an endothermic reaction[148], thus, the high leaching temperature is favorable for the leaching process. According to the references as shown in **Table 3.1**, the optimum temperature should be less than 90°C to show its potentiality on commercial scale. Thus, the effect of temperature on the leaching efficiency is investigated from 45, 55 and 65 °C under the condition of 148 $mg \cdot mL^{-1}$ OAR, 100 mM H_2O_2, 30 $g \cdot L^{-1}$ pulp density and 120 W ultrasonication for 60 minutes, and the result is shown in **Figure 3.5b.** The leaching efficiency of Li and Co increases as the increasing temperature due to temperature provides the energy to the molecule and increases the progress of reaction. When the temperature is at 55 °C, leaching efficiency of 47% for Co and 79% for Li are achieved at 60 minutes, this represents that OAR has a strong leaching ability even under mild temperature. When the temperature approaches to 65°C, 99% for Li and 86% for Co can be observed. Considering the energy consumption

and leaching efficiency, therefore, a fixing temperature of 65°C is proper for the rest investigations.

H_2O_2 has been widely used during the leaching process which provides one-valence oxygen atoms to convert Co (III) to Co (II) and strengthens the dissolution of Co(II).[126, 149] The effect of H_2O_2 concentration on the leaching efficiency is investigated and the result is shown in **Figure 3.5c.** The H_2O_2 dosage is varied from 0, 33, 100 and 140 mM under the condition of 148 $mg \cdot mL^{-1}$ OAR, 65°C temperature, 30 $g \cdot L^{-1}$ pulp density and 120 W ultrasonication for 60 minutes. H_2O_2, as a reducing agent, is unstable under high temperature and can be decomposed according to **Eq. (3.1).**[150]

$$2H_2O_2(aq) \rightarrow 2H_2O(aq)+O_2(g) \quad (3.1)$$

The reduction reaction changes the radius of cobalt ions which breaking the chemical bonds between Co and O and achieving leaching behavior further promoting the dissolution of Li.[151] Without the adding of reducing agent, around 45% for Co and 70% fo Li recovery efficiency can be achieved by OAR, showing that Li can dissolve in acid more easier than Co due to the weak interaction of Li within the layered LCO lattice,[152] and the strong leaching ability of OAR. As the concentration of H_2O_2 increases from 0 to 140 mM, the leaching efficiency increases from 45% to 94% for Co and 70% to 99% for Li respectively. H_2O_2 undergoes strong reaction under high temperature combining with

ultrasonication, which might lead to an unexpectable sever reaction such as the acid solution might split out causing safety issue, therefore, a dosage of 140 mM H_2O_2 is proper for the rest investigation.

The effect of the OAR concentration on the leaching efficiency is investigated from 148 , 90, 30 and 15 $mg \cdot mL^{-1}$ under the condition of 140 mM H_2O_2, 65°C temperature, 30 $g \cdot L^{-1}$ pulp density and 120 W ultrasonication, and the result is shown in **Figure 3.5d**. A leaching efficiency of 99% for Li and 94% for Co is achieved when the concentration of OAR is 148 $mg \cdot mL^{-1}$ in 60 minutes. As the concentration decreases from 148 to 15 $mg \cdot mL^{-1}$, a drastically decline from over 90% to under 10% for both Li and Co are observed in 60 minutes. This represents the leaching ability of OAR is weak, and almost lost the dissolution ability when the concentration is lower than 30 $mg \cdot mL^{-1}$. This may ascribe to the mechanism of OAR is worked by the principle of charge transfer in which the sulfur atom in $SOCl_2$ act as an electron acceptor, and the nitrogen in Py act as an electron donor.[131] This reaction release great energy to break the binding between Co and O when reacting with LCO, however, the excessive adding of H_2O will weaken this ability and break the OAR structures before the leaching experiment. Thus, to minimize the amount of input acid and to ensure the OAR works for the leaching experiment, we use 148 $mg \cdot mL^{-1}$ of OAR for the upcoming investigation.

Pulp density is the ratio of input OAR solution to the LCO, in which lower pulp density provides higher amount of OAR consumption to react with the LCO. The effect of

pulp density on the leaching efficiency is investigated from 30, 40 and 50 $g \cdot L^{-1}$ under the condition of 148 $mg \cdot mL^{-1}$ OAR, 65°C, 140 mM of H_2O_2 and 120 W ultrasonication for 60 minutes, and the result is shown in **Figure 3.5e.** The leaching efficiencies are increased from 52 to 99% for Li and 30 to 94% for Co while the pulp density decreasing from 50 to 30 $g \cdot L^{-1}$. This is due to less acid solution is reacted with the particles under high pulp density (40 and 50 $g \cdot L^{-1}$). Considering the lower OAR solution consumption and relatively better leaching efficiency, the optimal pulp density condition for Li and Co is 30 $g \cdot L^{-1}$.

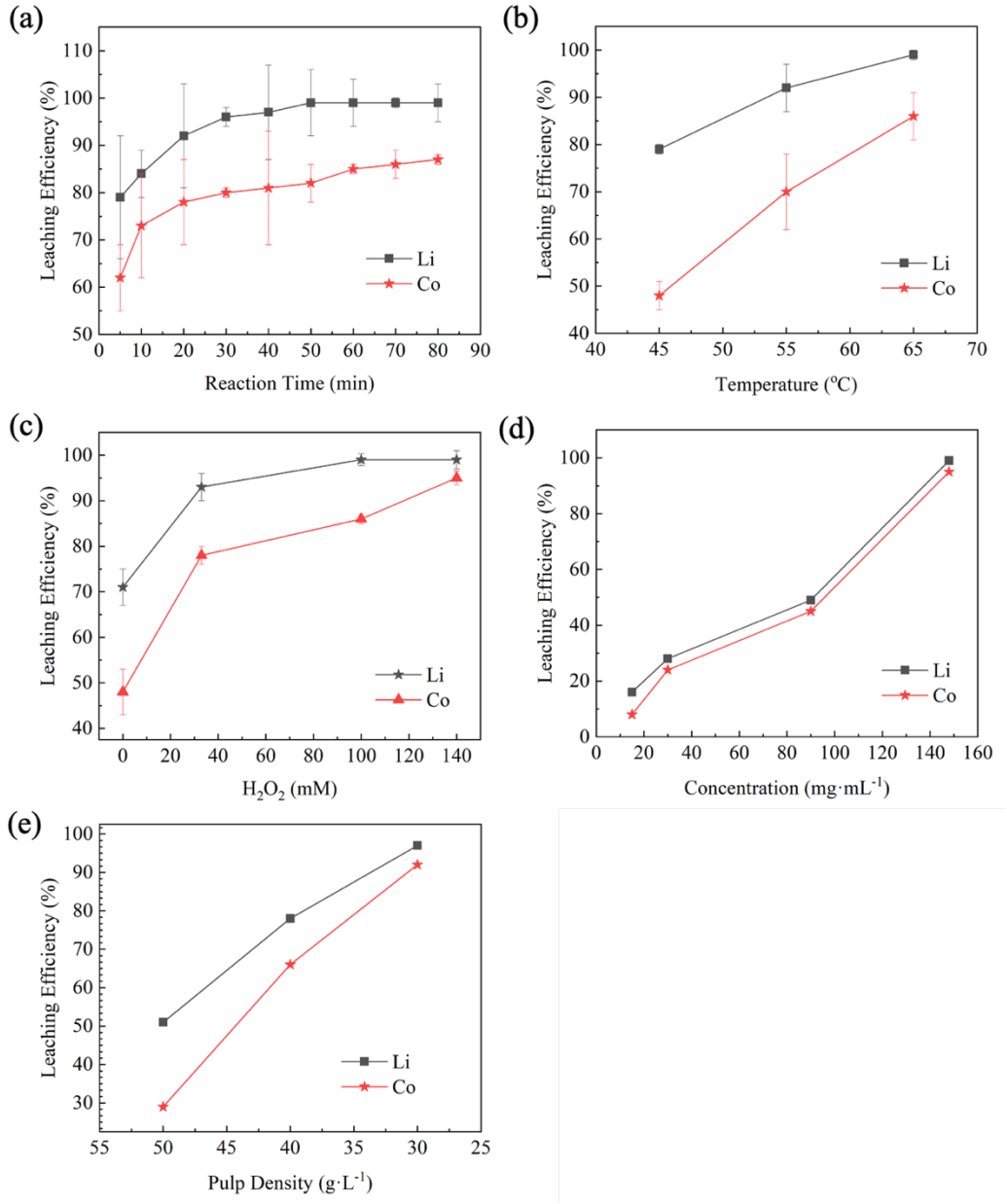

Figure 3.5 Leaching factors assessments for (a) effect of reaction on leaching efficiency ([H_2O_2]= 100mM, [OAR]= 148 mg·mL^{-1}, ultrasonication = 120W, T=65°C, 60 minutes)); (b) effect of temperature on leaching efficiency ([H_2O_2]= 100 mM, [OAR]= 148 mg·mL^{-1}, ultrasonication = 120W, pulp density= 30 g·L^{-1}, 60 minutes); (c) effect of H_2O_2 concentration on leaching efficiency. ([OAR]= 148 mg·mL^{-1}, T=65°C, ultrasonication = 120W, pulp density= 30 g·L^{-1}, 60 minutes);); (d) effect of concentration of OAR on leaching efficiency ([H_2O_2]= 140 mM, T=65°C, ultrasonication = 120 W, pulp density= 30 g·L^{-1}, 60 minutes); (e) effect of pulp density on leaching efficiency ([H_2O_2]= 140 mM, [OAR]= 148 mg·mL^{-1}, ultrasonication = 120W, T=65°C, 60 minutes).

3.3.1.2 Citric Acid and Nitric Acid

The results show that the leaching efficiencies are 95% for Li and 80% for Co of 1M citric acid, and 99% for Li and 80% for Co of 1M nitric acid under the same conditions of 100 mM H_2O_2, 65°C temperature, pulp density of 30g · L^{-1} for 60 minutes reaction time. In the **Figure 3.6**, a comparison of three acids in the study shows that OAR has the similar leaching efficiency with nitric acid, and a higher leaching efficiency than citric acid.

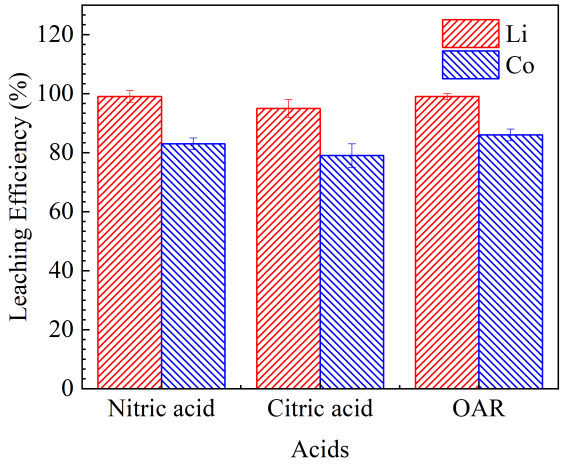

Figure 3.6 The comparison for three acids (1 M nitric acid, 1 M citric acid and 148 mg·mL^{-1} OAR) under the same condition ([H_2O_2]= 100 mM, T=65°C, ultrasonication = 120 W, pulp density= 30 g·L^{-1} for 60 minutes).

3.3.2 Dissolution Kinetic Study and Release Rate Determination

The dissolution kinetic study of Li and Co are studied with varied temperatures (45, 55, 65 °C) and leaching times (0-60 minutes) with 148 mg·mL^{-1} OAR. In **Figure 3.7**, the kinetic study of Li and Co both fit satisfactorily (R^2>0.92) to the chemical reaction model from 0 to 10 minutes, and fit satisfactorily (R^2>0.92) to the diffusion reaction model from 20 to 60 minutes. This provides the information that the progress is chemical control at the

beginning (0-10 minutes) due to high concentration of acid input under temperatures (45, 55, 65 °C)[28]. As the leaching progresses (20-60 minutes), the acid molecules have to diffuse through the layer to reach the reaction surface, which becomes diffusion control.[128]

Based on the dissolution rates provided in **Table 3.2**, the evolution of lnk with respect to the reverse of temperature, 1/T, the E_a values for leaching of Li and Co can be calculated from the slopes of the fitting lines. The values of the E_a for Li and Co are 12.3, 12.7 kJ·mol^{-1} for chemical reaction control, and 22.2 and 32.1 kJ·mol^{-1} for diffusion reaction control respectively, as shown in **Figure 3.8**. It is observed that both of the E_a values for Li are lower than Co, and E_a values for chemical reaction control are lower than for diffusion reaction control. In other words, leaching of Li is easier than leaching of Co[146] which is consistent with the experimental results represented in **Figure 3.5.** The relatively low E_a values for the chemical reaction control are indicative of the presence of H_2O_2 and good chelating ability of OAR which accelerate the leaching speed to transform the leaching behavior into surface chemical reaction control from 0 to 10 minutes. The reason may be ascribed that the leaching of Li is independent of any redox reaction process according to the literature.[129] Compared with other reported results from the literatures as shown in **Table 3.3,**[28, 129] the OAR shows relatively low Ea values of Li and Co for both chemical control and diffusion control, which may ascribe to the strong formation of donor-acceptor adducts inside OAR than other organic acids. [132]

Experimental release rate is calculated from the Li and Co leaching results which provides intuitional metals leaching release amount obtained from the leaching process as shown in **Figure 3.9**. The relatively high leaching release rate of 0.021, 0.167 $mg \cdot mg^{-1} \cdot h^{-1}$ for Li and Co than other reported data from the references which proves the distributed condition of E_a values in **Table 3.2.** The leaching behavior with OAR performs high release rate under the optimum experiment condition than others which can acts as potential candidates on the recovery of valuable metals from spent-LIBs and further mitigate the potential damage generated from the hydrometallurgy method by inorganic acids.

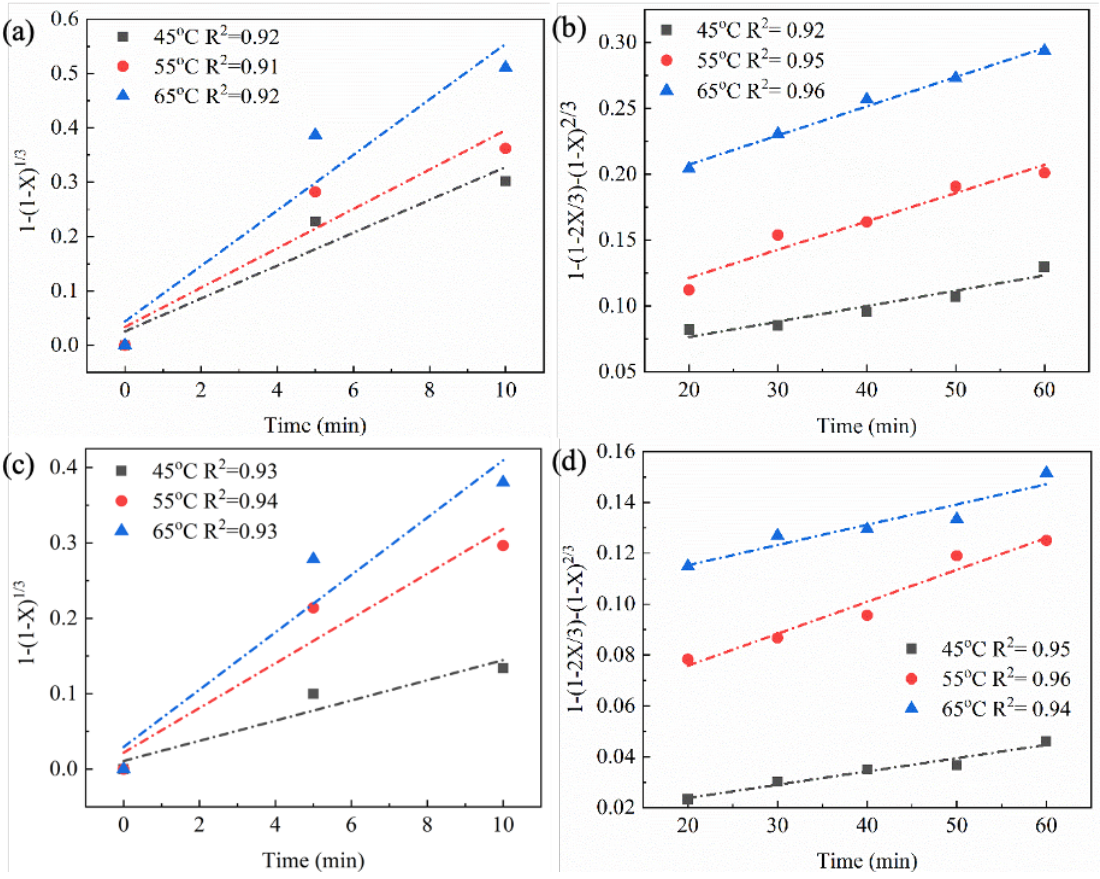

Figure 3.7 Plots of $1-(1-X)^{1/3}$ versus leaching time at temperature (45-65°C) by 148 $mg \cdot mL^{-1}$ for chemical reaction control (k_c): (a) Li and (b) Co; Plots of $1-(1-2X/3)-(1-X)^{2/3}$

versus leaching time at temperature (45-65°C) by 148 mg·mL^{-1} for dissolution reaction control (k_d): (c) Li and (d) Co.

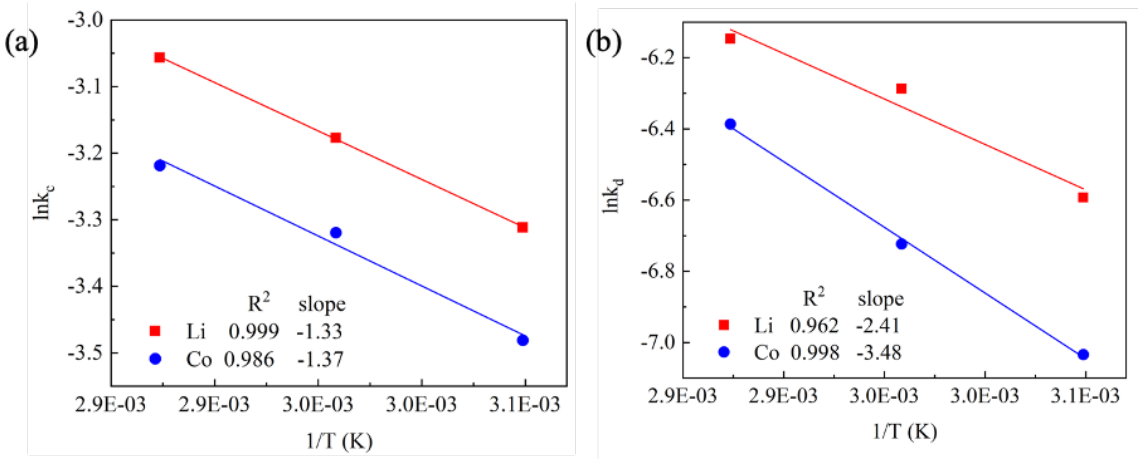

Figure 3.8 Arrhenius plot for Li and Co leaching for (a) under chemical reaction control (0-10 minutes) and (b) under diffusion reaction control (10-60 minutes).

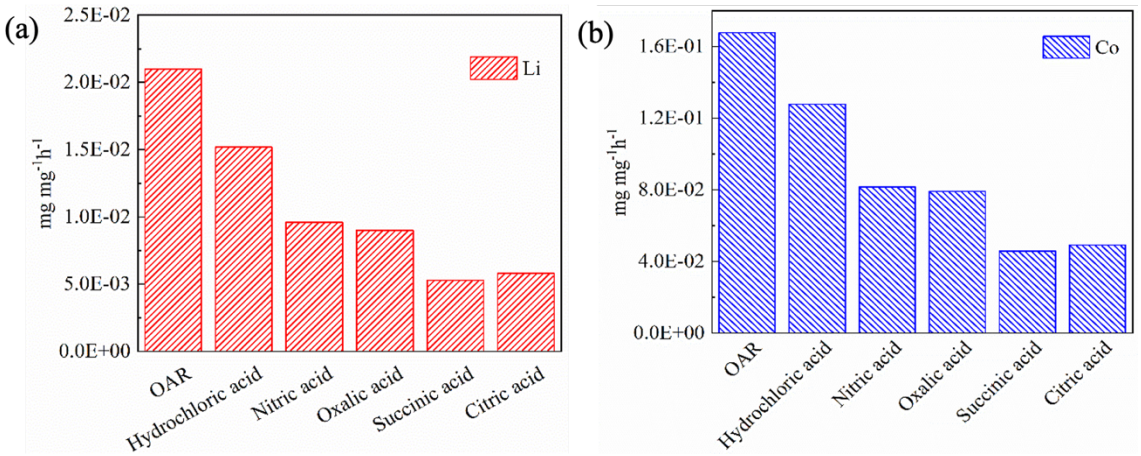

Figure 3.9 Leaching release rate bar graph of (a) Li and (b) Co by OAR in comparison with other reported results.

Table 3.2 Parameters of Dissolution Rate Constants for OAR Leachant

T (°C)	Chemical reaction control				Diffusion reaction control			
	Li k(min^{-1})	R^2	Co k(min^{-1})	R^2	Li k(min^{-1})	R^2	Co k(min^{-1})	R^2
45	0.0365	0.92	0.0308	0.93	0.0014	0.92	0.0009	0.95
55	0.0417	0.91	0.0362	0.94	0.0019	0.95	0.0012	0.96
65	0.0471	0.92	0.0401	0.93	0.0021	0.96	0.0017	0.94

Table 3.3 Comparison of E_a Values

Ref.		Chemical reaction				Diffusion reaction			
		Li		Co		Li		Co	
		E_a	R^2	E_a	R^2	E_a	R^2	E_a	R^2
unit		$kJ \cdot mol^{-1}$							
This study	OAR	11.1	0.99	11.4	0.96	20.1	0.96	28.9	0.99
[28]	1.2M Malic acid	20.3	0.99	29.9	0.98	22.6	0.99	31.2	0.99
[129]	3.5M Acetic acid	41.3	0.99	41.2	0.98	52.04	0.96	54.22	0.96
[128]	1M Malic acid	--	--	45.9	0.98	--	--	54.6	0.98
[128]	1M Citric acid	--	--	41.4	0.99	--	--	50.88	0.99
[25]	1.5M Succinic acid	8.9	0.91	13.6	0.95	25.94	0.95	--	--
[67]	1M Sulfuric acid	--	--	--	--	20.1	0.99	26.8	0.99
[18]	2 M Sulfuric acid	32.4	0.97	59.8	0.98	32.4	0.97	59.8	0.98

3.4 Life Cycle Assessment of Li and Co Recovery from Spent-LIBs

3.4.1 Life Cycle Assessment Emission Results

LCA emission results of 1 ton of LCO materials for the different recovery processes including Hydro-1 (sulfuric acid), Hydro-2 (citric acid), Hydro-3 (OAR), Pyro (pyrometallurgy method) and Virgin (total emission for the production of virgin $CoSO_4$). In **Fig. 3.10a** shows the result that recycling and recovering Li and Co from the spent-LIBs with Pyro and Hydro-1 save more than 50% GHG emission to produce a new LCO cathode materials for LIBs. This is better for the preservation of natural resources than extracting new virgin materials from mines because of the avoids of the significant SO_x emissions and save the energy consumption of CO_2 emission.[153] International Institute for Sustainable Development reported that the consumption of 500,000 gallons water resource and 31 to 89 $MJ \cdot kg^{-1}$ energy input[154, 155] when extracting 1 ton of virgin Li materials from Li-mine; consumption of 516,33 gallons water resource and 4.69 kWh energy (electricity, medium

voltage) when extracting 1 ton of virgin Co materials from Co mines.[156] However, the existing pyrometallurgy process cannot recover Li due to the high heating process from the smelter, and the hydrometallurgy method with inorganic acid has adverse impacts on both environment and human health. Currently, Hydrometallurgy methods with organic acids are uprising as an alternative way to recover Li and Co from spent-LIBs. **Fig. 3.10a** also indicates that Hydro-2 and Hydro-3 have over 60% of GHG emission reduction than extracting virgin materials from mines.

Furthermore, when comparing the energy consumption and emissions based on the four different recovery processes with quantification as shown in **Figure 3.10b.** The result shows Hydro-2 and Hydro-3 save 45% of GHG emission reduction than Pyro and Hydro-1. Hydrometallurgy with organic acids achieve greater energy savings, especially in electricity demand due to lack of slag process and long calcination duration in the pyrometallurgy process.[157] Hydro-2 and Hydro-3 based processes have similar emissions and air pollutant and GHG emissions are also less than Pyro and Hydro-1 due to organic acid utility. Among the emission factors, CO_2 emission is the most significant contributor for the environmental burden, and SO_x emission is the sub-contributor for the environmental burden. Detailed quantification information is listed in **Table 3.4** for the whole output emissions.

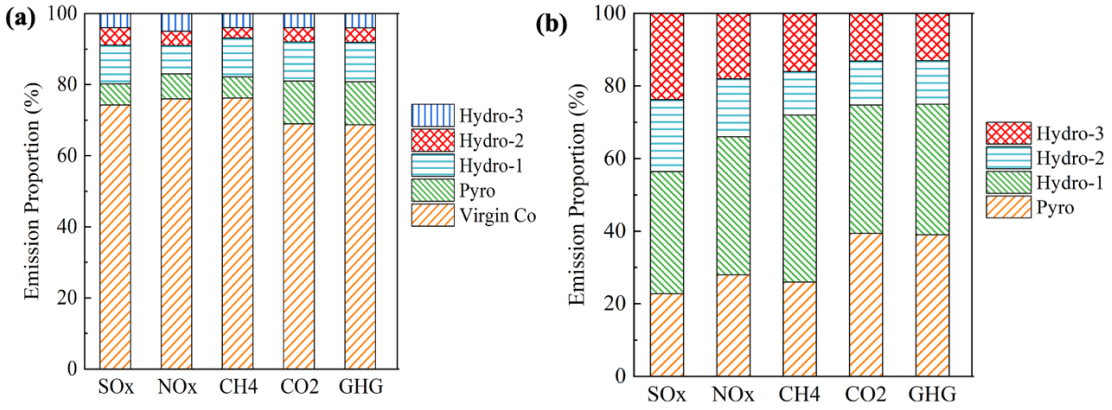

Figure 3.10 Comparison of main contribution emission proportion under different group base: (a) five different process including Hydro-1 (sulfuric acid), Hydro-2 (citric acid), Hydro-3 (OAR), Pyro (pyrometallurgy process) and Virgin (total emission for the production of virgin $CoSO_4$), (b) between four different recovery processes Hydro-1, Hydro-2, Hydro-3 and Pyro.

Table 3.4 Total Emission of Recovery Process

Ref. [140] kg per ton of LCO	Pyro [140]	Hydro-1 [140]	Hydro-2 [140]	This study Hydro-3	Virgin Co [140]
SO_x	14.9	22.3	13.3	17.7	73.8
NO_x	2.1	2.7	1.1	1.4	20.0
CH_4	2.4	4.3	1.1	1.5	30.5
CO_2	2277.7	2044.7	720.2	886.2	13035.1
GHG	2357.1	2185.9	763.0	906.7	13175.3

3.4.2 Life Cycle Assessment Emission Sensitivity Analysis

In order to quantify the influences brought about by input parameters, a sensitivity analysis is conducted.[158] The results of sensitivity analysis of hydrometallurgy process with OAR after the end-of-use GHG emissions are presented in **Figure 3.11.** The horizonal bars describe the variation in the kg GHG emission per ton of LCO for each experiment process. From **Figure 3.11,** variations in discharge and dismantle and heating system have significant attributions to the GHG emissions. Obviously, increasing the time of heating

system can lead to higher GHG emissions which is ascribed to the great CO_2 emission during the heating as a high-power instrument. However, this is a research-based lab-scale recovering process, large variations in heating system and discharge and dismantle might result from each part of the process has not being optimized as the industrial scale. Therefore, this lab-scale process results in a high emission estimation on both two stages mentioned previously. Simulation methods are further used to investigate the influence of uncertain parameters on sustainability indicators introduced above. To achieve this, Monte Carlo Simulations are conducted using the Oracle Crystal Ball add-in for excel. Each simulation consists of 100,000 Monte Carlo runs where for each run, Crystal Ball randomly selects input parameters based on predefined probability distributions, used to develop GHG emissions probability distributions. Input parameters are listed in **Table 3.5**.

Figure 3.12 shows that probability distributions have 90% confident intervals, besides, GHG emissions with the highest bars representing the values of the highest probabilities. The profile of log-distribution results from the nonlinear relationship between the input parameters and the lower probabilities of upper bound GHG emissions. Moreover, GHG emission significantly changes following with the variation of input parameters. Therefore, to apply optimizing and simple recovering process including the heating system can lead to more environmentally sustainable development. The information related to recovering process including discharge and dismantle, heating system, leaching solution, transportation and ultrasonication system. A potential future direction of this research is to

investigate ultrasonication assisted hydrometallurgy process with organic acids including OAR, citric acid under large industrial scale with specific defined experiment framework.

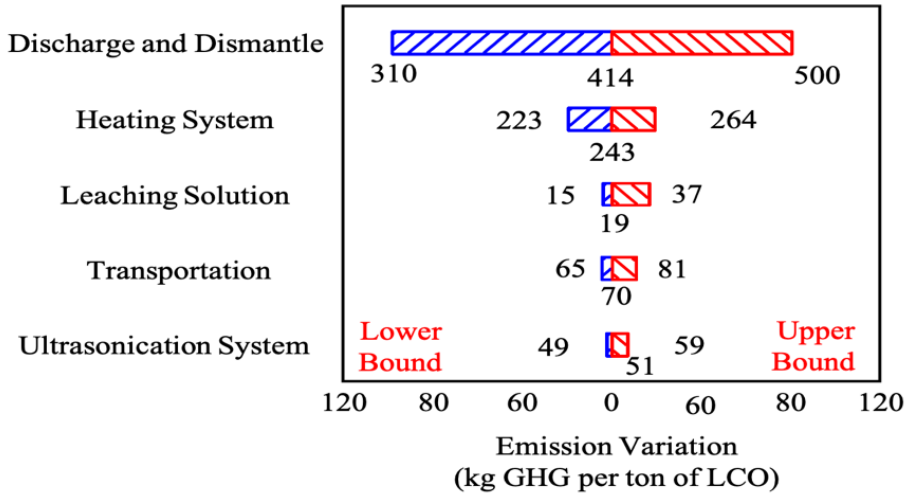

Figure 3.11 Emissions Variation of Hydrometallurgy process with OAR after the end of the use. The ranges for each input parameter are presented on the figure while the bars represent the variations in GHG emissions as input parameters are varied from their mean values.

Table 3.5 Ranges, Mean Values, and Sources of Input Parameters from the Self-report OAR Hydrometallurgy Process

Input Parameter Unit	Lower bound	Mean Value kg GHG per ton of LCO	Upper Bound
Discharge and Dismantle	310.691	414.633	500.207
Heating System	223.632	243.964	264.295
Leaching Solution	14.148	18.580	36.528
Transportation	64.722	69.574	80.901
Ultrasonication System	48.792	51.232	58.551

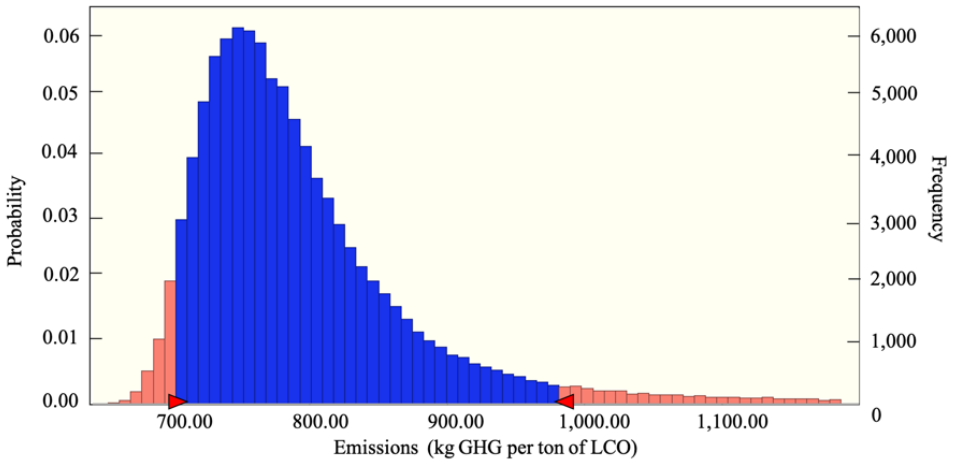

Figure 3.12 Emission distribution of process-based GHG emissions for LCO type LIBs OAR hydrometallurgy method. The 90% confident region is shown as the blue part.

3.4.3 The Social Cost of Carbon Pollution

Greenhouse gases emissions (GHG) such as SO_2, NO_2 and CO_2 have been recognized as the main attributions to the global climate change, which has received significant attention. Global climate change causes many devastating problems such as extreme weather events, the spread of disease and increased food insecurity. They bring a lot of cost toward the individual, families, businesses and governments. Among GHG, CO_2 is considered as the prominent gas which plays an important role on the impacts of environmental policy and research interest. A lot of attempts for researchers to identify and implement carbon mitigation and reduction strategies. Emissions are a negative externality from the harmful side effect of fuels burning. Without a price for each emission gas, emitters are not charged for releasing them into the atmosphere and have no incentive to reduce emissions. [159] Also, the earth's atmosphere we are living in is a public good, both non-rivalrous and non-excludable. The social cost of carbon (SCC) is the marginal cost of the impacts, in dollars,

of the economic damages that would result from emitting one extra ton of greenhouse gases into the atmosphere at any point in time[160], which is currently used by local, state, and federal governments to inform policy and investment decisions in the United States and abroad.

Figure 3.13 represent the estimation of social cost used in Federal regulatory analyses to value emissions changes occurring in certain years. The SCC increases over time because future emissions are expected to produce larger incremental damages as physical and economic systems become more stressed in response to greater climatic change. [161] The discount rate used in estimating the SCC incorporates both empirical evidence and value judgements. Under the base of **Figure 3.13,** we further adapt three different ways to get Li and Co materials, as listed in **Table 3.4**. To give an insight between cost and benefit when the company choose to replace current used pyrometallurgy to hydrometallurgy and even to an ultrasonication assisted hydrometallurgy method. Besides, this provides us strong incentive to recover Li and Co from the spent-LIBs rather than extract them from mining industry. Finally, in the **Figure 3.14**, we can use the SCC to calculate costs and benefits of changing emissions, and to compare the total economic benefits of a proposed policy to its total economic costs. The calculated results show that high benefit of $318.32 is achieved when complementing policy D to replace the original one. The benefit and cost according to the SCC may varied with the optimization of the system such as novel technology, better source generation when compared with existing

coal generation or from different calculated models with different factors(populations, economics growth, health, sea level rise and so on).

Discount Rate	5%	3%	2.5%	3%
Year	Avg	Avg	Avg	95th
2010	4.7	21.4	35.1	64.9
2015	5.7	23.8	38.4	72.8
2020	6.8	26.3	41.7	80.7
2025	8.2	29.6	45.9	90.4
2030	9.7	32.8	50.0	100.0
2035	11.2	36.0	54.2	109.7
2040	12.7	39.2	58.4	119.3
2045	14.2	42.1	61.7	127.8
2050	15.7	44.9	65.0	136.2

Figure 3.13 Social Cost of CO_2, 2010 – 2050 (per ton of CO_2 in 2007 dollars).

[161]

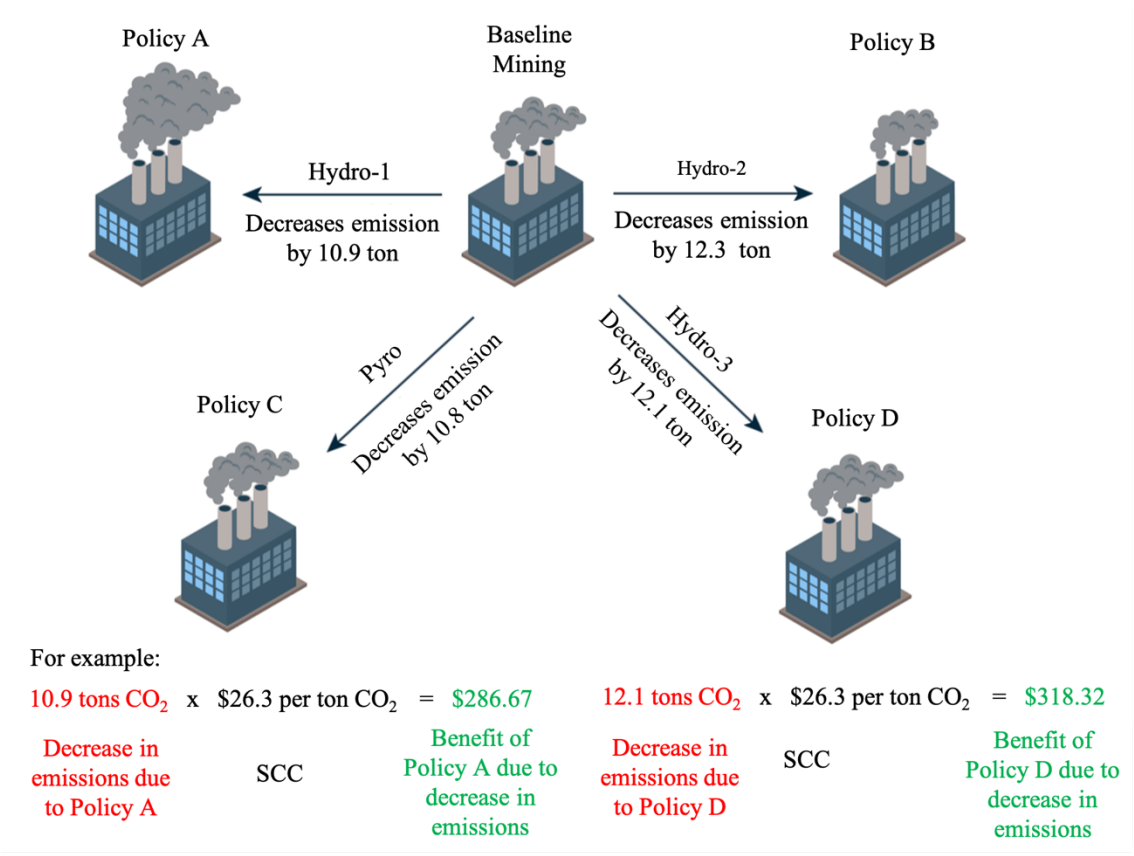

Figure 3.14 The costs and benefits of changing emissions by using SCC in 2020.

CONCLUSION

Lithium ion batteries (LIBs) are used in diverse electronic products with the market growth from $37.4 billion in 2018 to $58.8 billion by 2024. Accordingly, the quantity and weight of discarded waste LIBs in 2020 can surpass 25 billion units and 500 thousand tonnes, which release metals and toxic organic solvents and may negatively affect the environment and human health. To protect the environment and also recover valuable materials such as Li and Co that are categorized as strategically important materials by the US DoD, many chemical and material recovery programs, businesses, and research are booming up globally. Particularly, Li and Co recovery has been extensively studied through different processes such as pyrometallurgy, bio-hydrometallurgy and hydrometallurgy. Our research employed hydrometallurgy method using inorganic and organic acids (e.g., citric acids and nitric acid) and systematically compared the recovery efficiencies.

The results show that exposure of spent LIBs to 148 $mg \cdot mL^{-1}$ OAR and 140 mM H_2O_2 under 65^{o}C temperature, at a pulp density of 30 $g \cdot L^{-1}$ with the assistance of ultrasonication (120 W) could leach Li and Co without the pre-separation of cathode from Al foil using organic solvents such as Dimethylformamide (DMF) and N-Methyl-2-pyrrolidone (NMP). The leaching efficiency of 99% and 94% for Li and Co were obtained with a leaching rate of 0.021, 0.167 $mg \cdot mg^{-1} \cdot h^{-1}$ respectively. These data provide intuitional metals leaching release amount obtained from the whole hydrometallurgy process. OAR was significantly effective because of its strong chelating ability and high solubility in

water. The H_2O_2 concentration are approved to have significantly influence on the Li and Co recovery.

Dissolution rate constant analysis reveals that leaching processes is dominated by the chemical reaction in 10 minutes with the E_a value of 11.1 and 11.4 $kJ \cdot mol^{-1}$ for Li and Co, respectively. However, the leaching processes is dominated by the diffusion reaction at 20-60 minutes with the E_a value of 20.1 and 28.9 $kJ \cdot mol^{-1}$ for Li and Co, respectively. Compared with other reported results from the literatures, the OAR shows relatively low Ea values of Li and Co for both chemical control and diffusion control, which may ascribe to the strong formation of donor-acceptor adducts inside OAR reagent[132] than other organic acids. The process may promise an effective and environmentally friendly pathway for the recovery of valuable metals from spent-LIBs.

Finally, an LCA analysis is conducted for the emission and cost during the hydrometallurgy process with OAR. The LCA result of OAR show a reduction of 65% GHG emission than extraction from mine, a reduction of around 45% GHG emission than pyrometallurgy process and hydrometallurgy process with sulfuric acid and almost the same GHG emission condition as hydrometallurgy process with citric acid. The results of sensitivity analysis of hydrometallurgy process with OAR showing that variations in recovering process and heating consumption have significant attributions to the GHG emissions. Therefore, to apply optimizing and simple recovering process including the heating consumption can lead to more environmentally sustainable development.

This research aimed at improving the recovery processes of LIBs by reducing processing time, the use of hazardous pretreatment solvents and inorganic acid and prevention of pollution production or disposal (e.g., corrosive acid vapors). Moreover, our results provided new insight into the alternative organic acidic leaching with potential of acid recovery and reuse.

REFERENCES

1. Whittingham, M. S., Lithium Batteries and Cathode Materials. *Chemical Reviews* **2004,** *104* (10), 4271-4302.
2. Mizushima, K.; Jones, P. C.; Wiseman, P. J.; Goodenough, J. B., LixCoO2 (0<x<-1): A new cathode material for batteries of high energy density. *Materials Research Bulletin* **1980,** *15* (6), 783-789.
3. Ozawa, K., Lithium-ion rechargeable batteries with LiCoO2 and carbon electrodes: the LiCoO2/C system. *Solid State Ionics* **1994,** *69* (3), 212-221.
4. He, L.-P.; Sun, S.-Y.; Song, X.-F.; Yu, J.-G., Recovery of cathode materials and Al from spent lithium-ion batteries by ultrasonic cleaning. *Waste Management* **2015,** *46*, 523-528.
5. Eckart, J., Batteries can be part of the fight against climate change - if we do these five things. Inclusive Business Strategies, Global Leadership Fellow, World Economic Forum Geneva: 2017; pp https://www.weforum.org/agenda/2017/11/battery-batteries-electric-cars-carbon-sustainable-power-energy/.
6. Toma, C. M.; Ghica, G. V.; Buzatu, M.; Petrescu, M. I.; Vasile, E.; Iacob, G., A Recovery Process of Active Cathode Paste from Spent Li-Ion Batteries. *IOP Conference Series: Materials Science and Engineering* **2017,** *209* (1), 012034.
7. Market, R. a. "Lithium-Ion Battery Market Research Report: By Type, Application, Regional Insight - Global Industry Analysis and Forecast to 2024".
8. Research, W., < Lithium Ion Battery (Li-NMC, LFP, LCO, LTO, LMO, NCA) Market - Global Forecast to 2024_ High Energy Density Boosts the Demand for Li-NMC.pdf>. **2018**.
9. Lithium Ion Battery Market Size, Share and Forecast 2024: By Components, Product, Application,Sales and Segmentation -Tesla, Samsung,Philips.
10. Ordoñez, J.; Gago, E. J.; Girard, A., Processes and technologies for the recycling and recovery of spent lithium-ion batteries. *Renewable and Sustainable Energy Reviews* **2016,** *60*, 195-205.
11. Wang, X.; Gaustad, G.; Babbitt, C. W.; Bailey, C.; Ganter, M. J.; Landi, B. J., Economic and environmental characterization of an evolving Li-ion battery waste stream. *Journal of Environmental Management* **2014,** *135*, 126-134.
12. Vikström, H.; Davidsson, S.; Höök, M., Lithium availability and future production outlooks. *Applied Energy* **2013,** *110*, 252-266.
13. Xu, J.; Thomas, H. R.; Francis, R. W.; Lum, K. R.; Wang, J.; Liang, B., A review of processes and technologies for the recycling of lithium-ion secondary batteries. *Journal of Power Sources* **2008,** *177* (2), 512-527.
14. al, T. P. H. e., Life-cycle implications and supply chain logistics of electric vehicle battery recycling in California. Environ. Res. Lett. 10 014011, 2015

15. Zhang, X.; Xue, Q.; Li, L.; Fan, E.; Wu, F.; Chen, R., Sustainable Recycling and Regeneration of Cathode Scraps from Industrial Production of Lithium-Ion Batteries. *ACS Sustainable Chemistry & Engineering* **2016,** *4* (12), 7041-7049.
16. Golmohammadzadeh, R.; Faraji, F.; Rashchi, F., Recovery of lithium and cobalt from spent lithium ion batteries (LIBs) using organic acids as leaching reagents: A review. *Resources, Conservation and Recycling* **2018,** *136*, 418-435.
17. Chen, X.; Chen, Y.; Zhou, T.; Liu, D.; Hu, H.; Fan, S., Hydrometallurgical recovery of metal values from sulfuric acid leaching liquor of spent lithium-ion batteries. *Waste Management* **2015,** *38*, 349-356.
18. Jha, M. K.; Kumari, A.; Jha, A. K.; Kumar, V.; Hait, J.; Pandey, B. D., Recovery of lithium and cobalt from waste lithium ion batteries of mobile phone. *Waste Management* **2013,** *33* (9), 1890-1897.
19. Wang, R.-C.; Lin, Y.-C.; Wu, S.-H., A novel recovery process of metal values from the cathode active materials of the lithium-ion secondary batteries. *Hydrometallurgy* **2009,** *99* (3), 194-201.
20. Joulié, M.; Laucournet, R.; Billy, E., Hydrometallurgical process for the recovery of high value metals from spent lithium nickel cobalt aluminum oxide based lithium-ion batteries. *Journal of Power Sources* **2014,** *247*, 551-555.
21. Li, L.; Chen, R.; Sun, F.; Wu, F.; Liu, J., Preparation of LiCoO2 films from spent lithium-ion batteries by a combined recycling process. *Hydrometallurgy* **2011,** *108* (3), 220-225.
22. Lee, C. K.; Rhee, K.-I., Preparation of LiCoO2 from spent lithium-ion batteries. *Journal of Power Sources* **2002,** *109* (1), 17-21.
23. Chen, X.; Guo, C.; Ma, H.; Li, J.; Zhou, T.; Cao, L.; Kang, D., Organic reductants based leaching: A sustainable process for the recovery of valuable metals from spent lithium ion batteries. *Waste Management* **2018,** *75*, 459-468.
24. Chen, X.; Luo, C.; Zhang, J.; Kong, J.; Zhou, T., Sustainable Recovery of Metals from Spent Lithium-Ion Batteries: A Green Process. *ACS Sustainable Chemistry & Engineering* **2015,** *3* (12), 3104-3113.
25. Li, L.; Ge, J.; Wu, F.; Chen, R.; Chen, S.; Wu, B., Recovery of cobalt and lithium from spent lithium ion batteries using organic citric acid as leachant. *Journal of Hazardous Materials* **2010,** *176* (1), 288-293.
26. Li, L.; Qu, W.; Zhang, X.; Lu, J.; Chen, R.; Wu, F.; Amine, K., Succinic acid-based leaching system: A sustainable process for recovery of valuable metals from spent Li-ion batteries. *Journal of Power Sources* **2015,** *282*, 544-551.
27. Bahaloo-Horeh, N.; Mousavi, S. M., Enhanced recovery of valuable metals from spent lithium-ion batteries through optimization of organic acids produced by Aspergillus niger. *Waste Management* **2017,** *60*, 666-679.

28. Sun, C.; Xu, L.; Chen, X.; Qiu, T.; Zhou, T., Sustainable recovery of valuable metals from spent lithium-ion batteries using DL-malic acid: Leaching and kinetics aspect. *Waste Management & Research* **2017,** *36* (2), 113-120.
29. Li, L.; Ge, J.; Chen, R.; Wu, F.; Chen, S.; Zhang, X., Environmental friendly leaching reagent for cobalt and lithium recovery from spent lithium-ion batteries. *Waste Management* **2010,** *30* (12), 2615-2621.
30. Roshanfar, M.; Golmohammadzadeh, R.; Rashchi, F., An environmentally friendly method for recovery of lithium and cobalt from spent lithium-ion batteries using gluconic and lactic acids. *Journal of Environmental Chemical Engineering* **2019,** *7* (1), 102794.
31. Smith, K. A., Electrochemical Control of Lithium-Ion Batteries [Applications of Control]. *IEEE Control Systems Magazine* **2010,** *30* (2), 18-25.
32. Schröder, R.; Aydemir, M.; Seliger, G., Comparatively Assessing different Shapes of Lithium-ion Battery Cells. *Procedia Manufacturing* **2017,** *8*, 104-111.
33. Blomgren, G., The Development and Future of Lithium Ion Batteries. *Journal of The Electrochemical Society* **2017/01/01,** *164*.
34. Luzendu, G. C., Recovery of Lithium from Spent Lithium Ion Batteries.
35. Shukla, A.; Kumar, P., *Materials for Next-Generation Lithium Batteries*. 2008; Vol. 94.
36. Georgi-Maschler, T.; Friedrich, B.; Weyhe, R.; Heegn, H.; Rutz, M., Development of a recycling process for Li-ion batteries. *Journal of Power Sources* **2012,** *207*, 173-182.
37. Mekonnen, Y.; Sundararajan, A.; Sarwat, A. I. In *A review of cathode and anode materials for lithium-ion batteries*, SoutheastCon 2016, 30 March-3 April 2016; 2016; pp 1-6.
38. Chen, T.; Jin, Y.; Lv, H.; Yang, A.; Liu, M.; Chen, B.; Xie, Y.; Chen, Q., Applications of Lithium-Ion Batteries in Grid-Scale Energy Storage Systems. *Transactions of Tianjin University* **2020**.
39. Liu, P.; Xiao, L.; Chen, Y.; Chen, H., Highly enhanced electrochemical performances of LiNi0.815Co0.15Al0.035O2 by coating via conductively LiTiO2 for lithium-ion batteries. *Ceramics International* **2019,** *45* (15), 18398-18405.
40. Subhan, A.; Oemry, F.; Khusna, S. N.; Hastuti, E., Effects of activated carbon treatment on Li4Ti5O12 anode material synthesis for lithium-ion batteries. *Ionics* **2019,** *25* (3), 1025-1034.
41. Lavoie, Y.; Danet, F.; Lombard, B. In *Lithium-ion batteries for industrial applications*, 2017 Petroleum and Chemical Industry Technical Conference (PCIC), 18-20 Sept. 2017; 2017; pp 283-290.
42. Methekar, R.; Anwani, S. In *Manufacturing of Lithium Cobalt Oxide from Spent Lithium-Ion Batteries: A Cathode Material*, Innovations in Infrastructure,

Singapore, 2019//; Deb, D.; Balas, V. E.; Dey, R., Eds. Springer Singapore: Singapore, 2019; pp 233-241.
43. Ghatak, K.; Basu, S.; Das, T.; Sharma, V.; Kumar, H.; Datta, D., Effect of cobalt content on the electrochemical properties and structural stability of NCA type cathode materials. *Physical Chemistry Chemical Physics* **2018,** *20* (35), 22805-22817.
44. Ding, Y.; Cano, Z. P.; Yu, A.; Lu, J.; Chen, Z., Automotive Li-Ion Batteries: Current Status and Future Perspectives. *Electrochemical Energy Reviews* **2019,** *2* (1), 1-28.
45. Park, K.-J.; Hwang, J.-Y.; Ryu, H.-H.; Maglia, F.; Kim, S.-J.; Lamp, P.; Yoon, C. S.; Sun, Y.-K., Degradation Mechanism of Ni-Enriched NCA Cathode for Lithium Batteries: Are Microcracks Really Critical? *ACS Energy Letters* **2019,** *4* (6), 1394-1400.
46. Leisegang, T.; Meutzner, F.; Zschornak, M.; Münchgesang, W.; Schmid, R.; Nestler, T.; Eremin, R. A.; Kabanov, A. A.; Blatov, V. A.; Meyer, D. C., The Aluminum-Ion Battery: A Sustainable and Seminal Concept? *Frontiers in Chemistry* **2019,** *7* (268).
47. Deng, Z., Mo, Yifei.,Ong, Shyue, Computational studies of solid-state alkali conduction in rechargeable alkali-ion batteries. *NPG Asia Materials* **2016/03/25,** *8*.
48. Goodenough, J. B.; Kim, Y., Challenges for Rechargeable Li Batteries. *Chemistry of Materials* **2010,** *22* (3), 587-603.
49. Santen, D. C., Battery recycling pattern. *US pattern* **2005**.
50. Richardson, P. M.; Voice, A. M.; Ward, I. M., Pulsed-Field Gradient NMR Self Diffusion and Ionic Conductivity Measurements for Liquid Electrolytes Containing LiBF4 and Propylene Carbonate. *Electrochimica Acta* **2014,** *130*, 606-618.
51. Pal, P.; Ghosh, A., Dynamics and relaxation of charge carriers in poly(methylmethacrylate)-based polymer electrolytes embedded with ionic liquid. *Physical Review E* **2015,** *92* (6), 062603.
52. Liu, J.; Liu, Y.; Yang, W.; Ren, Q.; Li, F.; Huang, Z., Lithium ion battery separator with high performance and high safety enabled by tri-layered SiO2@PI/m-PE/SiO2@PI nanofiber composite membrane. *Journal of Power Sources* **2018,** *396*, 265-275.
53. Weber, C. J.; Geiger, S.; Falusi, S.; Roth, M., Material review of Li ion battery separators. *AIP Conference Proceedings* **2014,** *1597* (1), 66-81.
54. Patry, G.; Romagny, A.; Martinet, S.; Froelich, D., Cost modeling of lithium-ion battery cells for automotive applications. *Energy Science & Engineering* **2015,** *3* (1), 71-82.

55. Scott, A. In the battery materials world, the anode's time has come (https://cen.acs.org/materials/energy-storage/battery-materials-world-anodes-time/97/i14).
56. Huang, X., Separator technologies for lithium-ion batteries. *Journal of Solid State Electrochemistry* **2011,** *15* (4), 649-662.
57. IEA *Global EV Outlook 2019*; IEA, May 27 2019.
58. United States Lithium ion Battery Market By Type (Lithium Cobalt Oxide, Lithium Nickel Manganese Cobalt Oxide, etc.), By End Use (Consumer Electronics, Renewable Based ESS, etc.), By Battery Capacity, Competition Forecast & Opportunities, 2013 - 2023. **2018**.
59. Melin, H. E. *The lithium-ion battery end-of-life market-A baseline study*; 2018.
60. Zeng, X.; Li, J.; Singh, N., Recycling of Spent Lithium-Ion Battery: A Critical Review. *Critical Reviews in Environmental Science and Technology* **2014,** *44* (10), 1129-1165.
61. Daniel Cheret, S. B.; Sven Santen, H. S. Battery Recycling. 2007.
62. Liang, Y.; Su, J.; Xi, B.; Yu, Y.; Ji, D.; Sun, Y.; Cui, C.; Zhu, J., Life cycle assessment of lithium-ion batteries for greenhouse gas emissions. *Resources, Conservation and Recycling* **2017,** *117*, 285-293.
63. Sommer, P.; Rotter, V. S.; Ueberschaar, M., Battery related cobalt and REE flows in WEEE treatment. *Waste Management* **2015,** *45*, 298-305.
64. Tanskanen, P., Management and recycling of electronic waste. *Acta Materialia* **2013,** *61* (3), 1001-1011.
65. Yang, S.; Zhang, F.; Ding, H.; He, P.; Zhou, H., Lithium Metal Extraction from Seawater. *Joule* **2018,** *2* (9), 1648-1651.
66. Kim, J. H.; Gibb, H. J.; Howe, P. D.; World Health Organization. Chemical Safety, T.; International Programme on Chemical, S., Cobalt and inorganic cobalt compounds / prepared by James H. Kim, Herman J. Gibb, Paul D. Howe. World Health Organization: Geneva, 2006.
67. KATWALA, A. The spiralling environmental cost of our lithium battery addiction（https://www.wired.co.uk/article/lithium-batteries-environment-impact）.
68. Meshram, P.; Pandey, B.; Mankhand, T., Hydrometallurgical processing of spent lithium ion batteries (LIBs) in the presence of a reducing agent with emphasis on kinetics of leaching. *Chemical Engineering Journal* **2015,** *281*, 418-427.
69. Zheng, R.; Zhao, L.; Wang, W.; Liu, Y.; Ma, Q.; Mu, D.; Li, R.; Dai, C., Optimized Li and Fe recovery from spent lithium-ion batteries via a solution-precipitation method. *RSC Advances* **2016,** *6* (49), 43613-43625.
70. Nayaka, G. P.; Manjanna, J.; Pai, K. V.; Vadavi, R.; Keny, S. J.; Tripathi, V. S., Recovery of valuable metal ions from the spent lithium-ion battery using aqueous

mixture of mild organic acids as alternative to mineral acids. *Hydrometallurgy* **2015,** *151*, 73-77.

71. Yu, M.; Zhang, Z.; Xue, F.; Yang, B.; Guo, G.; Qiu, J., A more simple and efficient process for recovery of cobalt and lithium from spent lithium-ion batteries with citric acid. *Separation and Purification Technology* **2019,** *215*, 398-402.
72. Zheng, Y.; Long, H. L.; Zhou, L.; Wu, Z. S.; Zhou, X.; You, L.; Yang, Y.; Liu, J. W., Leaching Procedure and Kinetic Studies of Cobalt in Cathode Materials from Spent Lithium Ion Batteries using Organic Citric acid as Leachant. *International Journal of Environmental Research* **2016,** *10* (1), 159-168.
73. Nayaka, G. P.; Zhang, Y.; Dong, P.; Wang, D.; Zhou, Z.; Duan, J.; Li, X.; Lin, Y.; Meng, Q.; Pai, K. V.; Manjanna, J.; Santhosh, G., An environmental friendly attempt to recycle the spent Li-ion battery cathode through organic acid leaching. *Journal of Environmental Chemical Engineering* **2019,** *7* (1), 102854.
74. Gao, W.; Liu, C.; Cao, H.; Zheng, X.; Lin, X.; Wang, H.; Zhang, Y.; Sun, Z., Comprehensive evaluation on effective leaching of critical metals from spent lithium-ion batteries. *Waste Management* **2018,** *75*, 477-485.
75. Meshram, P.; Pandey, B.; Mankhand, T., Recovery of valuable metals from cathodic active material of spent lithium ion batteries: leaching and kinetic aspects. *Waste Management* **2015,** *45*, 306-313.
76. Sun, L.; Qiu, K., Organic oxalate as leachant and precipitant for the recovery of valuable metals from spent lithium-ion batteries. *Waste Management* **2012,** *32* (8), 1575-1582.
77. Zhang, X.; Cao, H.; Xie, Y.; Ning, P.; An, H.; You, H.; Nawaz, F., A closed-loop process for recycling LiNi1/3Co1/3Mn1/3O2 from the cathode scraps of lithium-ion batteries: Process optimization and kinetics analysis. *Separation and Purification Technology* **2015,** *150*, 186-195.
78. Yang, L.; Xi, G.; Xi, Y., Recovery of Co, Mn, Ni, and Li from spent lithium ion batteries for the preparation of LiNixCoyMnzO2 cathode materials. *Ceramics International* **2015,** *41* (9, Part A), 11498-11503.
79. Yao, L.; Feng, Y.; Xi, G., A new method for the synthesis of LiNi1/3Co1/3Mn1/3O2 from waste lithium ion batteries. *RSC Advances* **2015,** *5* (55), 44107-44114.
80. Song, D.; Wang, X.; Zhou, E.; Hou, P.; Guo, F.; Zhang, L., Recovery and heat treatment of the Li(Ni1/3Co1/3Mn1/3)O2 cathode scrap material for lithium ion battery. *Journal of Power Sources* **2013,** *232*, 348-352.
81. Weng, Y.; Xu, S.; Huang, G.; Jiang, C., Synthesis and performance of Li[(Ni1/3Co1/3Mn1/3)1−xMgx]O2 prepared from spent lithium ion batteries. *Journal of Hazardous Materials* **2013,** *246-247*, 163-172.

82. Zhou, X.; He, W.; Li, G.; Zhang, X.; Zhu, S.; Huang, J.; Zhu, S. In *Recycling of Electrode Materials from Spent Lithium-Ion Batteries*, 2010 4th International Conference on Bioinformatics and Biomedical Engineering, 18-20 June 2010; 2010; pp 1-4.
83. Zhang, X.; Xie, Y.; Cao, H.; Nawaz, F.; Zhang, Y., A novel process for recycling and resynthesizing LiNi1/3Co1/3Mn1/3O2 from the cathode scraps intended for lithium-ion batteries. *Waste Management* **2014,** *34* (9), 1715-1724.
84. Junmin Nanz, D. H., Minjie Yang and Ming Cui, Dismantling, Recovery, and Reuse of Spent Nickel–Metal Hydride Batteries. *J. Electrochem. Soc* **2006**.
85. Chen, L.; Tang, X.; Zhang, Y.; Li, L.; Zeng, Z.; Zhang, Y., Process for the recovery of cobalt oxalate from spent lithium-ion batteries. *Hydrometallurgy* **2011,** *108* (1), 80-86.
86. Ferreira, D. A.; Prados, L. M. Z.; Majuste, D.; Mansur, M. B., Hydrometallurgical separation of aluminium, cobalt, copper and lithium from spent Li-ion batteries. *Journal of Power Sources* **2009,** *187* (1), 238-246.
87. Nan, J.; Han, D.; Yang, M.; Cui, M.; Hou, X., Recovery of metal values from a mixture of spent lithium-ion batteries and nickel-metal hydride batteries. *Hydrometallurgy* **2006,** *84* (1), 75-80.
88. Nan, J.; Han, D.; Zuo, X., Recovery of metal values from spent lithium-ion batteries with chemical deposition and solvent extraction. *Journal of Power Sources* **2005,** *152*, 278-284.
89. Li, J.; Shi, P.; Wang, Z.; Chen, Y.; Chang, C.-C., A combined recovery process of metals in spent lithium-ion batteries. *Chemosphere* **2009,** *77* (8), 1132-1136.
90. Li, L.; Zhai, L.; Zhang, X.; Lu, J.; Chen, R.; Wu, F.; Amine, K., Recovery of valuable metals from spent lithium-ion batteries by ultrasonic-assisted leaching process. *Journal of Power Sources* **2014,** *262*, 380-385.
91. Jie, L. B. C. H.-q. G., Research progress on dewatering performance of municipal excess sludge pretreated by ultrasonic. *Industrial water and wastewater* **2017,** *48(04),1-6*.
92. Wang, J.; Wang, Z.; Vieira, C. L. Z.; Wolfson, J. M.; Pingtian, G.; Huang, S., Review on the treatment of organic pollutants in water by ultrasonic technology. *Ultrasonics Sonochemistry* **2019,** *55*, 273-278.
93. Hanisch, C.; Loellhoeffel, T.; Diekmann, J.; Markley, K. J.; Haselrieder, W.; Kwade, A., Recycling of lithium-ion batteries: a novel method to separate coating and foil of electrodes. *Journal of Cleaner Production* **2015,** *108*, 301-311.
94. Yang, Y.; Huang, G.; Xu, S.; He, Y.; Liu, X., Thermal treatment process for the recovery of valuable metals from spent lithium-ion batteries. *Hydrometallurgy* **2016,** *165*, 390-396.

95. Cui, J.; Forssberg, E., Mechanical recycling of waste electric and electronic equipment: a review. *Journal of Hazardous Materials* **2003,** *99* (3), 243-263.
96. Zhang, T.; He, Y.; Wang, F.; Ge, L.; Zhu, X.; Li, H., Chemical and process mineralogical characterizations of spent lithium-ion batteries: An approach by multi-analytical techniques. *Waste Management* **2014,** *34* (6), 1051-1058.
97. Shin, S. M.; Kim, N. H.; Sohn, J. S.; Yang, D. H.; Kim, Y. H., Development of a metal recovery process from Li-ion battery wastes. *Hydrometallurgy* **2005,** *79* (3), 172-181.
98. Pan, L.; Jung, S.; Yoon, R. H., Effect of hydrophobicity on the stability of the wetting films of water formed on gold surfaces. *Journal of Colloid and Interface Science* **2011,** *361* (1), 321-330.
99. Liu, J.; Wang, H.; Hu, T.; Bai, X.; Wang, S.; Xie, W.; Hao, J.; He, Y., Recovery of LiCoO2 and graphite from spent lithium-ion batteries by cryogenic grinding and froth flotation. *Minerals Engineering* **2020,** *148*, 106223.
100. Zhan, R.; Oldenburg, Z.; Pan, L., Recovery of active cathode materials from lithium-ion batteries using froth flotation. *Sustainable Materials and Technologies* **2018,** *17*, e00062.
101. Xiao, J.; Li, J.; Xu, Z., Recycling metals from lithium ion battery by mechanical separation and vacuum metallurgy. *Journal of Hazardous Materials* **2017,** *338*, 124-131.
102. Lee, C. K.; Rhee, K.-I., Reductive leaching of cathodic active materials from lithium ion battery wastes. *Hydrometallurgy* **2003,** *68* (1), 5-10.
103. Meng, Q.; Zhang, Y.; Dong, P., Use of glucose as reductant to recover Co from spent lithium ions batteries. *Waste Management* **2017,** *64*, 214-218.
104. Martínez, P.; Orozco, J.; Alonso-Gómez, A.; Luna, R.; Barron, M.; Medina, D.; Garfias-García, E., Lithium Recovery from Electrodes in Cellphone Batteries through the Leaching Process with Organic Agents Assisted by Ultrasound. *Journal of Materials Science and Chemical Engineering* **2018,** *06*, 1-5.
105. Jiang, F.; Chen, Y.; Ju, S.; Zhu, Q.; Zhang, L.; Peng, J.; Wang, X.; Miller, J., Ultrasound-assisted Leaching of Cobalt and Lithium from Spent Lithium-ion Batteries. *Ultrasonics Sonochemistry* **2018,** *48*.
106. Meshram, P.; Pandey, B. D.; Mankhand, T. R., Recovery of valuable metals from cathodic active material of spent lithium ion batteries: Leaching and kinetic aspects. *Waste Management* **2015,** *45*, 306-313.
107. Träger, T.; Friedrich, B.; Weyhe, R., Recovery Concept of Value Metals from Automotive Lithium-Ion Batteries. *Chemie Ingenieur Technik* **2015,** *87* (11), 1550-1557.
108. Zhang, G.; He, Y.; Wang, H.; Feng, Y.; Xie, W.; Zhu, X., Application of mechanical crushing combined with pyrolysis-enhanced flotation technology to

recover graphite and LiCoO2 from spent lithium-ion batteries. *Journal of Cleaner Production* **2019,** *231*, 1418-1427.

109. Hu, J.; Zhang, J.; Li, H.; Chen, Y.; Wang, C., A promising approach for the recovery of high value-added metals from spent lithium-ion batteries. *Journal of Power Sources* **2017,** *351*, 192-199.
110. Bahaloo-Horeh, N.; Mousavi, S. M.; Baniasadi, M., Use of adapted metal tolerant Aspergillus niger to enhance bioleaching efficiency of valuable metals from spent lithium-ion mobile phone batteries. *Journal of Cleaner Production* **2018,** *197*, 1546-1557.
111. Hagelüken, C., *Recycling of Electronic Scrap at Umicore. Precious Metals Refining*. 2006; Vol. 12, p 111-120.
112. Deng, X.; Chai, L.; Yang, Z.; Tang, C.; Wang, Y.; Shi, Y., Bioleaching mechanism of heavy metals in the mixture of contaminated soil and slag by using indigenous Penicillium chrysogenum strain F1. *Journal of Hazardous Materials* **2013,** *248-249*, 107-114.
113. Heydarian, A.; Mousavi, S. M.; Vakilchap, F.; Baniasadi, M., Application of a mixed culture of adapted acidophilic bacteria in two-step bioleaching of spent lithium-ion laptop batteries. *Journal of Power Sources* **2018,** *378*, 19-30.
114. Huang, T.; Liu, L.; Zhang, S., Recovery of cobalt, lithium, and manganese from the cathode active materials of spent lithium-ion batteries in a bio-electro-hydrometallurgical process. *Hydrometallurgy* **2019,** *188*, 101-111.
115. Boxall, N. J.; Cheng, K. Y.; Bruckard, W.; Kaksonen, A. H., Application of indirect non-contact bioleaching for extracting metals from waste lithium-ion batteries. *Journal of Hazardous Materials* **2018,** *360*, 504-511.
116. Naseri, T.; Bahaloo-Horeh, N.; Mousavi, S. M., Environmentally friendly recovery of valuable metals from spent coin cells through two-step bioleaching using Acidithiobacillus thiooxidans. *Journal of Environmental Management* **2019,** *235*, 357-367.
117. Mishra, D.; Kim, D.-J.; Ralph, D. E.; Ahn, J.-G.; Rhee, Y.-H., Bioleaching of metals from spent lithium ion secondary batteries using Acidithiobacillus ferrooxidans. *Waste Management* **2008,** *28* (2), 333-338.
118. Lambert, F.; Gaydardzhiev, S.; Léonard, G.; Lewis, G.; Bareel, P.-F.; Bastin, D., Copper leaching from waste electric cables by biohydrometallurgy. *Minerals Engineering* **2015,** *76*, 38-46.
119. Martínez-Bussenius, C.; Navarro, C. A.; Jerez, C. A., Microbial copper resistance: importance in biohydrometallurgy. *Microbial Biotechnology* **2017,** *10* (2), 279-295.
120. Werner, A.; Meschke, K.; Bohlke, K.; Daus, B.; Haseneder, R.; Repke, J.-U., Resource Recovery from Low-Grade Ore Deposits and Mining Residuals by

Biohydrometallurgy and Membrane Technology. Potentials and Case Studies. *ChemBioEng Reviews* **2018,** *5* (1), 6-17.

121. Dutta, D.; Kumari, A.; Panda, R.; Jha, S.; Gupta, D.; Goel, S.; Jha, M. K., Close loop separation process for the recovery of Co, Cu, Mn, Fe and Li from spent lithium-ion batteries. *Separation and Purification Technology* **2018,** *200*, 327-334.
122. Novikov, G. V.; Vikent'ev, I. V.; Mel'nikov, M. E.; Bogdanova, O. Y.; Eremin, N. I., Cobalt, nickel, and copper in ore minerals of cobalt-bearing ferromanganese crusts from the Magellan Seamounts of the Pacific Ocean. *Doklady Earth Sciences* **2013,** *450* (1), 566-570.
123. Niu, Z.; Zou, Y.; Xin, B.; Chen, S.; Liu, C.; Li, Y., Process controls for improving bioleaching performance of both Li and Co from spent lithium ion batteries at high pulp density and its thermodynamics and kinetics exploration. *Chemosphere* **2014,** *109*, 92-98.
124. Horeh, N. B.; Mousavi, S. M.; Shojaosadati, S. A., Bioleaching of valuable metals from spent lithium-ion mobile phone batteries using Aspergillus niger. *Journal of Power Sources* **2016,** *320*, 257-266.
125. Fu, Y.; He, Y.; Qu, L.; Feng, Y.; Li, J.; Liu, J.; Zhang, G.; Xie, W., Enhancement in leaching process of lithium and cobalt from spent lithium-ion batteries using benzenesulfonic acid system. *Waste Management* **2019,** *88*, 191-199.
126. Ning, P.; Meng, Q.; Dong, P.; Duan, J.; Xu, M.; Lin, Y.; Zhang, Y., Recycling of cathode material from spent lithium ion batteries using an ultrasound-assisted DL-malic acid leaching system. *Waste Management* **2020,** *103*, 52-60.
127. Chen, X.; Kang, D.; Cao, L.; Li, J.; Zhou, T.; Ma, H., Separation and recovery of valuable metals from spent lithium ion batteries: Simultaneous recovery of Li and Co in a single step. *Separation and Purification Technology* **2018,** *210*.
128. Musariri, B.; Akdogan, G.; Dorfling, C.; Bradshaw, S., Evaluating organic acids as alternative leaching reagents for metal recovery from lithium ion batteries. *Minerals Engineering* **2019,** *137*, 108-117.
129. Gao, W.; Song, J.; Cao, H.; Zhang, X.; Hong, Z.; Zhang, Y.; Sun, Z. H. I., Selective recovery of valuable metals from spent lithium-ion batteries – Process development and kinetics evaluation. *Journal of Cleaner Production* **2018,** *178*.
130. Lin, W.; Zhang, R. W.; Jang, S. S.; Wong, C. P.; Hong, J. I., "Organic aqua regia"--powerful liquids for dissolving noble metals. *Angew Chem Int Ed Engl* **2010,** *49* (43), 7929-32.
131. Lin, W.; Zhang, R.-W.; Jang, S.-S.; Wong, C.-P.; Hong, J.-I., "Organic Aqua Regia"—Powerful Liquids for Dissolving Noble Metals. *Angewandte Chemie International Edition* **2010,** *49* (43), 7929-7932.

132. Serpe, A.; Marchiò, L.; Artizzu, F.; Mercuri, M. L.; Deplano, P., Effective One-Step Gold Dissolution Using Environmentally Friendly Low-Cost Reagents. *Chemistry – A European Journal* **2013,** *19* (31), 10111-10114.
133. Yun, L.; Linh, D.; Shui, L.; Peng, X.; Garg, A.; Le, M. L. P.; Asghari, S.; Sandoval, J., Metallurgical and mechanical methods for recycling of lithium-ion battery pack for electric vehicles. *Resources, Conservation and Recycling* **2018,** *136*, 198-208.
134. Sicklinger, J.; Metzger, M.; Beyer, H.; Pritzl, D.; Gasteiger, H. A., Ambient Storage Derived Surface Contamination of NCM811 and NCM111: Performance Implications and Mitigation Strategies. J. Electrochem.: 2019; Vol. Soc. 2019 volume 166, issue 12, A2322-A2335.
135. Zheng, X.; Gao, W.; Zhang, X.; He, M.; Lin, X.; Cao, H.; Zhang, Y.; Sun, Z., Spent lithium-ion battery recycling – Reductive ammonia leaching of metals from cathode scrap by sodium sulphite. *Waste Management* **2017,** *60*, 680-688.
136. Liu, B.; Huang, Q.; Su, Y.; Sun, L.; Wu, T.; Wang, G.; Kelly, R. M.; Wu, F., Maleic, glycolic and acetoacetic acids-leaching for recovery of valuable metals from spent lithium-ion batteries: leaching parameters, thermodynamics and kinetics. *Royal Society Open Science 6* (9), 191061.
137. Curran, M. A., Life-Cycle Assessment. In *Encyclopedia of Ecology*, Jørgensen, S. E.; Fath, B. D., Eds. Academic Press: Oxford, 2008; pp 2168-2174.
138. Muralikrishna, I. V.; Manickam, V., Chapter Five - Life Cycle Assessment. In *Environmental Management*, Muralikrishna, I. V.; Manickam, V., Eds. Butterworth-Heinemann: 2017; pp 57-75.
139. RingstrSm, J. W. a. E., life cycle assessment. 2007.
140. Systems, E.; Laboratory, A. N., GREET2, 2019(https://greet.es.anl.gov). 2019.
141. Finkbeiner, M.; Inaba, A.; Tan, R.; Christiansen, K.; Klüppel, H.-J., The New International Standards for Life Cycle Assessment: ISO 14040 and ISO 14044. *The International Journal of Life Cycle Assessment* **2006,** *11* (2), 80-85.
142. Call2Recycle, I. https://www.call2recycle.org/start-recycling/.
143. Recycling NJ Battery.
144. Call2Recycle, I. h. w. c. r. o. p. s.-b.-c.-r.-b.
145. Administration, U. S. D. o. T.-F. H. Compilation of Existing State Truck Size and Weight Limit Laws(https://ops.fhwa.dot.gov/freight/policy/rpt_congress/truck_sw_laws/app_a.htm).
146. Fu, Y.; He, Y.; Chen, H.; Ye, C.; Lu, Q.; Li, R.; Xie, W.; Wang, J., Effective leaching and extraction of valuable metals from electrode material of spent lithium-ion batteries using mixed organic acids leachant. *Journal of Industrial and Engineering Chemistry* **2019,** *79*, 154-162.

147. Chen, X.; Fan, B.; Xu, L.; Zhou, T.; Kong, J., An Atom-economic Process for the Recovery of High Value-added Metals from Spent Lithium-ion Batteries. *Journal of Cleaner Production* **2015,** *112*.
148. Nayl, A. A.; Elkhashab, R. A.; Badawy, S. M.; El-Khateeb, M. A., Acid leaching of mixed spent Li-ion batteries. *Arabian Journal of Chemistry* **2017,** *10*, S3632-S3639.
149. Yu, M.; Zhang, Z.; Xue, F.; Yang, B.; Guo, G.; Qiu, J., *A more simple and efficient process for recovery of cobalt and lithium from spent lithium-ion batteries with citric acid*. 2019; Vol. 215.
150. Zhang, X.; Xie, Y.; Lin, X.; Li, H.; Cao, H., An overview on the processes and technologies for recycling cathodic active materials from spent lithium-ion batteries. *Journal of Material Cycles and Waste Management* **2013,** *15* (4), 420-430.
151. Pinna, E. G.; Ruiz, M. C.; Ojeda, M. W.; Rodriguez, M. H., Cathodes of spent Li-ion batteries: Dissolution with phosphoric acid and recovery of lithium and cobalt from leach liquors. *Hydrometallurgy* **2017,** *167*, 66-71.
152. Yang, Y.; Xu, S.; He, Y., Lithium recycling and cathode material regeneration from acid leach liquor of spent lithium-ion battery via facile co-extraction and co-precipitation processes. *Waste Management* **2017,** *64*, 219-227.
153. Gaines, L.; Sullivan, J.; Burnham, A., Paper No. 11-3891 Life-Cycle Analysis for Lithium-Ion Battery Production and Recycling. *Transportation Research Board 90th Annual Meeting, Washington, DC* **2011**.
154. Church, C.; Wuennenberg, L., Sustainability and Second Life: The case for cobalt and lithium recycling. International Institute for Sustainable Development: March 2019.
155. Ambrose, H.; Kendall, A., Understanding the future of lithium: Part 2, temporally and spatially resolved life-cycle assessment modeling. *Journal of Industrial Ecology* **2019,** *n/a* (n/a).
156. Farjana, S. H.; Huda, N.; Mahmud, M. A. P., Life cycle assessment of cobalt extraction process. *Journal of Sustainable Mining* **2019,** *18* (3), 150-161.
157. Georgi-Maschler, T.; Friedrich, B.; Weyhe, R.; Heegn, H.; Rutz, M., Development of a Recycling Process for Li-Ion Batteries. *Journal of Power Sources* **2012,** *207*, 173–182.
158. Yue, D.; Khatav, P.; You, F.; Darling, S. B., Deciphering the uncertainties in life cycle energy and environmental analysis of organic photovoltaics. *Energy & Environmental Science* **2012,** *5* (11), 9163-9172.
159. STRAIN, K. B. D. J. M., It Starts With a Social Cost of Carbon. **2019,** (The University of Chicago, Booth School of Business
The University of Chicago, Harris School of Public Policy).

160. al, P. e., Climate Change 2007: Impacts, Adaptation and Vulnerability. Contribution of Working Group II to the Fourth Assessment Report of the Intergovernmental Panel on Climate Chang. *Cambridge University Press* **2011**.
161. Council of Economic Advisers , C. o. E. Q., Department of Agriculture, Department of Commerce, Department of Energy, Department of Transportation, Environmental Protection Agency, National Economic Council,Office of Energy and Climate Change,Office of Management and Budget, Office of Science and Technology Policy, Department of the Treasury. *Technical Support Document: -Social Cost of Carbon for Regulatory Impact Analysis - Under Executive Order 12866* -; Interagency Working Group on Social Cost of Carbon, United States Government: 2010.
162. Holthoff, J. M.; Engelage, E.; Kowsari, A. B.; Huber, S. M.; Weiss, R., Noble Metal Corrosion: Halogen Bonded Iodocarbenium Iodides Dissolve Elemental Gold—Direct Access to Gold–Carbene Complexes. *Chemistry – A European Journal* **2019,** *0* (0).